Sex–specific Single Transcript Level Atlas of Vasopressin and its Receptor (AVPR1a) in the Mouse Brain

Anisa Gumerova, Georgii Pevnev, Funda Korkmaz, Uliana Cheliadinova, Guzel Burganova, Darya Vasilyeva, Liam Cullen, Orly Barak, Farhath Sultana, Weibin Zhou, Steven Sims, Emily Weiss, Victoria Laurencin, Tal Frolinger, Se-Min Kim, Ki A. Goosens, Tony Yuen, Mone Zaidi and Vitaly Ryu

Institute for Translational Medicine and Pharmacology, Icahn School of Medicine at Mount Sinai, New York, NY 10029

Corresponding Authors: Mone Zaidi [mone.zaidi@mssm.edu], Vitaly Ryu [vitaly.ryu@mssm.edu]

Abbreviated Title: Brain atlas of vasopressin and its Avpr1a receptor

Conflict of Interest: M.Z. is inventor on issued and pending patents on the use of FSH as a target for osteoporosis, obesity and Alzheimer's disease. M.Z. and T.Y. are inventors on a pending patent on an FSH antibody that is formulated at ultrahigh concentration. The patents will be held by Icahn School of Medicine at Mount Sinai, and M.Z. and T.Y. would be recipients of royalties, *per* institutional policy. The other authors declare no competing financial interests.

ABSTRACT

Vasopressin (AVP), a nonapeptide synthesized predominantly by magnocellular hypothalamic neurons, is conveyed to the posterior pituitary *via* the pituitary stalk, where AVP is secreted into the circulation. Known to regulate blood pressure and water homeostasis, it also modulates diverse social behaviors, such as pair–bonding, social recognition and cognition in mammals including humans. Importantly, AVP modulates social behaviors in a sex–specific manner, perhaps, due to sex differences in the distribution in the brain of AVP and its main receptor AVPR1a. There is a *corpus* of integrative studies for the expression of AVP and AVPR1a in various brain regions, and their functions in modulating central and peripheral actions. In order to purposefully address sexually dimorphic and novel roles of AVP on central and peripheral functions through its AVPR1a, we utilized RNAscope to map *Avp* and *Avpr1a* single transcript expression in the mouse brain. As the most comprehensive atlas of AVP and AVPR1a in the mouse brain, this compendium highlights the importance of newly identified AVP/AVPR1a neuronal nodes that may stimulate further functional studies.

INTRODUCTION

Vasopressin (AVP), a nonapeptide synthesized primarily by magnocellular neurons of the paraventricular nucleus (PVH) and supraoptic nucleus (SO) of the hypothalamus, is conveyed along axons of magnocellular neurons *via* the pituitary stalk to the posterior pituitary, where AVP is released into circulation to exert hormonal functions (1, 2). Involved in the regulation of blood pressure and water balance (3, 4), AVP also regulates diverse social behaviors, such as pair–bonding, social recognition and cognition in all mammals, including humans (5-9). It should be noted that similar to OXT, AVP is evolutionarily conserved across invertebrates and vertebrate taxa, differing from OXT by just only two amino acids. Importantly, AVP modulates social behaviors in sex–specific manner, perhaps due to sex differences in AVP and its receptor expression in the brain (10-15).

AVP receptors are G protein–coupled receptors consisting of two major subtypes, the V1 receptor (AVPR1) and V2 receptor (AVPR2) (16). AVPR1 has two subtypes, namely AVPR1a and AVPR1b that mediate the effects of AVP on social behaviors. Avpr1a will be the overarching focus of this study given its abundance and ubiquity in brain regions (9). In fact, differences in AVPR1a genetic variability and expression patterns determine specific social phenotypes (17-21). There is evidence that AVPR1a is involved in maternal care, pair–bonding, behavioral aggression, anxiety, social recognition and social play (6, 9, 19, 22-25). The sex–dependent distribution of Avpr1a across the brain in different species provides a proxy for the distribution of AVP binding, and therefore, provides further evidence for central AVP neural nodes of physiologic relevance.

Blocking AVPR1a inhibits social recognition in the rat, while AVPR1a knockout mice fail to display social recognition (15, 22, 26). These effects of AVP in enhancing social recognition is mediated *via* AVPR1a in the lateral septum (15, 26). Sex differences in Avpr1a binding densities have been described in several brain sites of Wistar rats. Namely, males display higher AVPR1a binding densities in the following forebrain areas: somatosensory and piriform cortex, medial posterior bed nucleus of the stria terminalis (BNST), nucleus of the lateral olfactory tract (LOT), anteroventral thalamic nucleus (VA), tuberal lateral hypothalamus (LH), stigmoid hypothalamus (Stg), and dentate gyrus (DG) (16). In male prairie voles, central AVP infusion facilitates selective aggression associated with pair bond formation and partner preferences, and the Avpr1a antagonist 1-(*β*-mercapto-*β, β*-cyclopentamethylene propionic acid) does not seem to inhibit aggression (10). In contrast, central AVP infusion induces a partner preference in female prairie voles (11). Comparative analysis of AVPR1a distribution has revealed higher densities of AVPR1a binding in the ventral pallidum, amygdala, and thalamus of prairie voles than that of meadow or montane voles (27, 28). It has also been reported that AVPR1a antagonism specifically in the ventral pallidum prevents mating–induced partner preferences in male prairie voles (29).

Although osmotically stimulated AVP release with short latency and duration from hypothalamic PVH and SO magnocellular axon terminals occurs in the pituitary (30, 31), it is also released locally from somata and dendrites in the SO with a longer delay responding to osmotic challenge (32, 33). Such local release is likely to facilitate autocrine and/or paracrine regulation of SO–magnocellular neuronal activity and inhibit further systemic AVP output (33, 34). Of note, somatodendritic AVP release in

response to direct hypertonic stimulation is attenuated by V1/V2 receptor antagonism, implying that AVP may facilitate its own release by acting on autoreceptors within magnocellular neurons of the SO (35). The importance of autofacilitation to local AVP release may lay in fine–tuned regulation of AVP actions towards physiologic demands. Alternatively, AVP could putatively diffuse over longer distances to bind to adjacent receptors. The relative contribution of AVP autoreceptor subtypes, including AVPR1a, to this phenomenon awaits further clarification.

Current studies implicate posterior pituitary hormones, traditionally thought of as master regulators of a single physiological target, in the control of multiple bodily systems, either directly or *via* their receptors in the brain (23, 36-39). Non–traditional actions of AVP include its ability to affect skeletal homeostasis, wherein it negatively regulates osteoblasts and stimulates osteoclasts. This explains the bone loss that accompanies low blood sodium levels in patients with high AVP levels (40). Furthermore, we have shown that AVP (via AVPR1a) and oxytocin (via OXTR) have opposing skeletal actions—effects that may relate to the pathogenesis of bone loss in chronic hyponatremia, and pregnancy and lactation, respectively (40-43).

Detecting specific AVPR1a and AVPR1b in the brain has had limitations for a long time due to the availability of only nonselective radioligands, such as tritium labeled (^{3}H) AVP ligands, which bind to both receptors (44). Although there is a large body of integrative studies for the expression of AVP and AVPR1a in various brain regions, and their functions in regulating central and peripheral actions, there remains the need for detailed, sex–specific mapping of the AVP/AVPR1a neuronal nodes in the brain. We utilized RNAscope—a technology that detects single RNA transcripts—to create a

comprehensive atlas of AVP and AVPR1a in the mouse brain. It may seem somewhat remarkable that newly discovered brain areas for receptors of such evolutionarily conserved and well–studied hormones AVP and OXT are currently emerging, with inferences to novel functions. We believe that this atlas of AVP and its AVPR1a in concrete brain sites at a single transcript level should provide a resource to neuroscientists to deepen our understanding of classical and novel central and peripheral functions of AVP by interrogating AVPR1a site–specifically.

RESULTS

AVP receptors are G protein-coupled receptors consisting of two major subtypes, the AVPR1 and AVPR2 (16). In turn, AVPR1 is divided into AVPR1a and AVPR1b receptor subtypes that mediate the effects of AVP in the brain on social behaviors. In this study, we have provided not only a distribution mapping of AVP and AVPR1a in the brain, but also assessed sex differences in their expression by RNAscope. Allowing the detection of single transcripts, RNAscope uses ~20 pairs of transcript–specific double *Z*–probes to hybridize 10–µm–thick whole brain sections. Preamplifiers first hybridize to the ~28–bp binding site formed by each double *Z*–probe; amplifiers then bind to the multiple binding sites on each preamplifier; and finally, labeled probes containing a chromogenic enzyme bind to multiple sites of each amplifier.

RNAscope data were quantified on every tenth section of the whole brains from coded 3 female and 3 male mice. For simplicity and clarity in the graphs, a scatter plot has been shown for 3 nuclei, sub–nuclei and regions with the highest AVP and AVPR1a

transcript densities as well as their absolute transcript counts. Each section was viewed and analyzed using CaseViewer 2.4 (3DHISTECH, Budapest, Hungary) and QuPath v.0.2.3 (University of Edinburgh, UK). The *Atlas for the Mouse Brain in Stereotaxic Coordinates* (45) was used to identify every nucleus, sub–nucleus or region, which was followed by manual counting of *Avp* and *Avpr1a* transcripts by two independent observers (V.R. and A.G.) in every tenth section using a tag feature. Receptor density was calculated by dividing the absolute receptor number by the total area (μm^2, ImageJ) of every nucleus, sub–nucleus or region. The highest *Avp* and *Avpr1a* values in the brain regions are presented as means ± SE and compared with those of the opposite sex. Photomicrographs were prepared using Photoshop CS5 (Adobe Systems) only to adjust brightness, contrast and sharpness, to remove artifacts (*i.e.*, obscuring bubbles), and to make composite plates.

RNAscope revealed *Avp* expression in the hypothalamus, forebrain, hippocampus and cortex of both female and male mice (Fig. 1A), however, *Avp* expression in the 3rd ventricular region and thalamus was found only in the female mouse (Fig. 1B). Whereas the numbers of *Avp*–expressing cells were greater in females compared with males in the hypothalamus (607 vs. 471), 3rd ventricular region (7 vs. 0) and thalamus (2 vs. 0), those numbers were lower in the hippocampus (58 vs. 118), forebrain (50 vs. 77) and cortex (5 vs. 6) [see Appendix 1 for Glossary and Supplementary Fig. 1 for raw count graphs].

The highest *Avp* transcript densities were detected in following brain nuclei, sub–nuclei and regions of female and male mice, respectively: ventricular region—3V only for females, hypothalamus—SChVL and PaDC, forebrain—MPOM and VLPO,

hippocampus—Py and GrDG, thalamus—ic only for females and cerebral cortex—Pir for both (Fig. 1B). Representative micrographs of some of the hypothalamic and forebrain regions with highest *Avp* expression are shown in Fig. 1C.

We found that *Avpr1a* transcript expression in several brain nuclei, for example, the MS of the forebrain, medullary IOBe, IRt, LRt (Supplementary Fig. 2B), displayed individual patterns of expression *vs.* a more ubiquitous and even expression noted in most of the other brain areas, suggesting brain–site–specific functional diversity and context–selective regulation of *Avpr1a*–mediated signaling. We report the expression of the *Avpr1a* in 398 and 375 brain nuclei, sub–nuclei and regions of the female and male mice, respectively. *Avpr1a* transcripts were detected bilaterally, with no apparent ipsilateral domination. Probe specificity was established by a positive signal in renal tubules of the kidney (positive control) with an absent signal in the FrA of the frontal cortex (negative control) (Fig. 2A). Representative micrographs of sex–specific medullary CC and hypothalamic Arc with highest *Avpr1a* expression also are shown in Fig. 2A.

In the female, total *Avpr1a* transcript numbers were the highest in the medulla followed, in descending order, by the hypothalamus, cortex, midbrain and pons, forebrain, thalamus, cerebellum, hippocampus, olfactory bulb and ventricular regions (Supplementary Fig. 2A). In the male, *Avpr1a* transcripts were the highest in the forebrain, followed by the medulla, midbrain and pons, hypothalamus, cortex, hippocampus, thalamus, olfactory bulb, cerebellum and ventricular regions (Supplementary Fig. 2).

Using the RNAscope dataset we further calculated *Avpr1a* density in all brain divisions (Fig. 2B), nuclei, sub–nuclei and regions (Fig. 2C). Highest *Avpr1a* densities in the female and male mice, respectively, were noted in nuclei, sub–nuclei and regions as follows: ventricular regions—CC ependymal region for both with 2.92–fold greater in the male; hypothalamus—Arc for both; medulla—IOBe and InM; midbrain and pons—vtgx and DRI; forebrain—AC and LSI; olfactory bulb—Mi and Tu; hippocampus—TS and df; thalamus—PV and Xi; cortex—MPtA and AID and cerebellum—1Cb for both with 2.58-fold greater in the female (Fig. 2C).

In addition, RNAscope analysis revealed that various brain nuclei, sub–nuclei and regions in both female and male mice co–localized *Avp* and *Avpr1a* transcripts. *Avpr1a* to *Avp* ratios within the same brain nucleus, sub–nucleus and region in both sexes are demonstrated in Figs. 3A, B. Finally, RNAscope showed *Avp* and *Avpr1a* expression in the posterior pituitary lobe with *Avp* and *Avpr1a* transcript densities that were higher in male compared with female mice, however, without statistical significance (Fig. 4).

DISCUSSION

Here, we attempted to integrate previous information on sex–specific AVP and its AVPR1a expression in the murine brain. AVPR1a is the most abundant and wide spread receptor in the brain (9) that plays a dominant role in regulating behavior. In addition, we focused towards paradigm–shifting non–traditional roles of central AVP signaling in light of newly discovered AVPR1a. We report AVP expression in 41 female and 13 male brain nuclei, sub–nuclei and regions. Moreover, we identified abundant

AVPR1a expression in 398 female and 375 male brain nuclei, sub–nuclei and regions. Therefore, this report is the most exhaustive atlas of brain *Avp* and *Avpr1a* expression at the single transcript level.

It has been reported that AVP synthesis and AVP fiber projections are sexually dimorphic in specific brain sites [for review, see: (16)]. To our knowledge, the first discovery of the sexually dimorphic nature of AVP in the rat brain was made by De Vries *et al*. (46). That is, males displayed more AVP–immunoreactive fibers in the lateral septum and lateral habenular nucleus over females (46). Surprisingly, sex differences in AVP fiber density in the LS and medial amygdala (MeA) originate from the BNST, given only lesions to the BNST, but not the PVH, result in decreased AVP fiber density in the LS (47, 48). In adult rats, AVP fiber density from the BNST and MeA are dependent on circulating gonadal hormones, as gonadectomy eliminates AVP expression and hormone replacement restores AVP fiber network (49, 50). Nonetheless, gonadal hormones appear to only partially explain sex difference in AVP expression because both females and males, exposed to a similar gonadal steroid hormone regime, still differ sexually (51, 52).

Magnocellular neurons of the PVN, SO and SCh of the hypothalamus are the predominant source of AVP synthesis. Hypothalamic AVP synthesis of most rodent species is similar between males and females in the PVH and SO of mice (53, 54); PVH, SO and SCh of voles (55, 56); PVH, MPOA, LH and AHA of Mongolian gerbils and Chinese striped hamsters (57) [for review, see: (16)]. In concordance with these reports, we also find no sex difference in *Avp* synthesis, as evidenced by similar numbers of *Avp*–expressing neurons, in the PVH and SO of mice; however, we did note sex

differences in *Avp* expression density in specific hypothalamic nuclei. Notably, *Avp* expression density was higher in several PVH (PaLM and PaMM) and suprachiasmatic (SChVL and RCh) subnuclei of female compared to male mice. No sex differences in SO–*Avp* expression density were found.

Furthermore, *Avpr1a* transcript density was highest in the arcuate nucleus (Arc) and retrochiasmatic sub–nucleus (RCh) in female compared with Arc and suprachiasmatic nucleus (SCh) of male mice. *Avpr1a* expression in the Arc has previously been reported (58), however, its role was unclear until a recent report demonstrating a critical involvement of Arc–NPY in the regulation of fluid homeostasis and the induction of salt water–induced hypertension through AVP modulation in the SO (59); the latter receives direct projections from the Arc (60). In contrast, it is plausible, but, by no means proven, that PVH– and/or SO–AVP may modulate Arc anorexigenic neurons to inhibit ingestive behavior, which has previously been shown with PVH oxytocinergic neurons (61). Indeed, increasing evidence suggests that AVP reduces feeding in mammals (62, 63).

It has been reported that in the rat, AVP is an important output of the SCh targeting AVP cells in other hypothalamic areas—its release into the CSF peaks in the early morning and declines later in a day (64). Specifically, SCh–AVP secreted during late sleep activates osmosensory afferents to AVP neurons in the SO and organum vasculosum of the lamina terminalis (65, 66). Similar to rodents, studies in humans also determined that the main AVP projections from the SCh target the anteroventral hypothalamic area, sub–PVH as well as ventral parts of the PVH and DMH—a remarkable evolutionary conservation of SCh innervation from rodent to human (67, 68).

The fact that the SCh is another brain nucleus with high AVP and AVPR1a expression density (greater in males vs. females), accentuates an important role of SCh–AVP in circadian rhythmicity, notably impacting neuroendocrine day/night rhythms, feeding timing, period, precision, and synchronization of SCh neurons (64, 69, 70).

In the hindbrain, the highest *Avpr1a* transcript density was noted in the inferior olive, beta subnucleus (IOBe) of female and intermedius nucleus (InM) of male mice. It has been reported that AVP fibers are apparent in the hindbrain, such as the parabrachial nucleus, locus coeruleus, and near inferior olive nuclei (71). In this regard, *Avpr1a* mRNA expression has been noted in the inferior olive (58). Given this nucleus has been implicated in various functions including learning and timing of movements, it is possible that AVPR1a in the inferior olive may be activated by the paracrine release of AVP from distant nuclei, such as the SCh, to control motor learning and timing. Alternatively, AVPR1a in the inferior olive may respond to other ligands (for example, OXT) found in nearby regions (72). The role of AVPR1 in the InM of male mice is less clear, but because the InM sends monosynaptic projections to the NTS (73) that is essential for blood pressure control by AVP and receiving information from the cardiovascular receptors (74), a possible coordinated control by hindbrain AVP of blood pressure and cardiovascular function.

Although the midbrain, pons and forebrain displayed less abundant *Avpr1a* transcript density, they revealed further sex differences. In the midbrain and pons, the highest *Avpr1a* density was in the ventral tegmental decussation (vtgx) in females and dorsal raphe nucleus, interfascicular part (DRI) in males. AVP and OXT in the ventral tegmental area are known to regulate social interactions with rewarding properties.

Indeed, humans, as inherently social beings, show a strong inclination to affiliate and share their emotions with each other (75, 76). Sex differences in ventral tegmental AVPR1a make biological sense, as social interaction of females, specifically, with pups and, generally, with counterparts throughout their lives, have rewarding properties fundamental to maternal behavior and survival. Modulation of AVPR1a in the dorsal raphe nucleus has also been linked to social and emotional behaviors (16, 77, 78). Sexual dimorphism in AVP innervation of and AVPR1a expression in the DRI appears to imprint dimorphic social behaviors. That is, AVPR1a blockade in the lateral habenular nucleus (LHb) of males, but not females who have lesser AVP innervation of the LHb and dorsal raphe nucleus, results in reduced urine marking to unfamiliar males and ultrasonic vocalizations to unfamiliar, sexually receptive females, whereas AVPR1a blockade in the dorsal raphe nucleus of only males reduces urine marking to unfamiliar males (77).

In the forebrain, both sexes displayed high *Avpr1a* transcript density in septal nuclei. The highest *Avpr1a* density was in the anterior commissural nucleus (AC) within the septal nuclei of females, and lateral (LSI) and medial (MS) septal nuclei of males. It is not surprising that *Avpr1a* transcript density was significantly greater in septal nuclei of males than females given in many rodent species males have more AVP–immunoreactive fibers in the lateral septum (46). Notably, the effects of AVP on social recognition is mediated *via* AVPR1a in the lateral septum (15, 26). For example, AVPR1a blockade inhibits social recognition in the rat, while AVPR1a knockout mice fail to display social recognition (15, 22, 26).

Despite *Avpr1a* transcript densities in other brain divisions were significantly lower, sexually dimorphic differences are worth mentioning here. In the olfactory bulb, females had the high *Avpr1a* density in the mitral cell layer (Mi), whereas males had high receptor expression in the olfactory tubercle (Tu). A population of AVP neurons in the olfactory bulb of the rat that play a role in social recognition via AVPR1a has been reported (79). Silencing the AVPR1a by siRNA impairs habituation/dishabituation to juvenile cues, but not to volatile odors (79). Of note, AVP is a retrograde signal that filters activation of the Mi cells in the ewe, likely through presynaptic modulation of norepinephrine or acetylcholine. The secretion of both transmitters is stimulated by AVP in the olfactory bulb (79, 80). The functional relevance of AVP signaling *via* AVPR1a activation in the Tu requires additional studies. There is, however, evidence in the rat that AVP *via* AVPR1a has, at least, an indirect impact on Tu function, as seen by a reduction in activation responding to a noxious odor of butyric acid, when the AVPR1a is blocked (81). The presence of AVPR1a in the hippocampus, thalamus, cortex, and ventricular regions are consistent with the reported effects of AVP on memory (82), emotional and reward–motivated behavior (83), blood pressure (84), blood flow and CSF production (85). Functional roles of many other nuclei shown here to express AVPR1a and not mentioned in this report are much less clear. The importance of revealing novel AVP–triggered functions by interrogating AVPR1a site–specifically, will require further investigations.

Collectively, our results provide compelling evidence of distinct and novel AVP/AVPR1a neuronal nodes in the brain. While studies on central AVP signaling and its control of blood pressure, water balance and diverse social behaviors in mammals,

occupy the vast majority of the literature (3-9), we expect that this comprehensive compendium of sex–specific AVP/AVPR1a expression in the brain will deepen our understanding of the functional and neuroanatomical basis underlying old and new paradigm–shifting functions of central AVP signaling. As appears to be the case for most brain areas, the original discovery of function tends to become dogma thereby leading to an oversimplification of multiple functions of those brain areas as they interact in circuits. Finally, the approach of direct mapping of receptor expression in the brain and periphery provides the groundwork for greater discernment of new functional arrangements of ancient pituitary glycoprotein hormones and nonapeptides, such as AVP and OXT, and provide helpful pointers towards improving pharmacological interventions in disease.

METHODS

Mice

Adult mice (~3 to 4–month–old) were housed in a 12 h:12 h light : dark cycle at 22 ± 2 ºC with *ad libitum* access to water and regular chow. All procedures were approved by the Mount Sinai Institutional Animal Care and Use Committee and are in accordance with Public Health Service and United States Department of Agriculture guidelines.

RNAscope

For RNAscope, mice were anesthetized with isoflurane (2-3% in oxygen; Baxter Healthcare, Deerfield, IL) and transcardially perfused with 0.9% heparinized saline followed by 10% Neutral Buffered Formalin (NBF). Brains were promptly extracted, post-fixed in 10% NBF for 24 h, dehydrated, and paraffin–embedded. Coronal sections were cut at 5 µm, with every tenth section mounted onto ~60 slides with 3 sections on each slide. This method allows to cover the entire brain and eliminate the likelihood of counting the same transcript twice. Sections were air-dried overnight at room temperature and stored at 4 °C until required.

Detection of mouse *Avp* and *Avpr* (*Avpr1a*) was performed separately on paraffin sections using Advanced Cell Diagnostics (ACD) RNAscope 2.5 LS Reagent Kit (#322100) and two RNAscope 2.5 LS probes, namely Mm-AVP-O1 (#472268) and Mm-AVPR1a (#418068). The kidney and prefrontal cortex served as positive and negative controls for AVPR1a, respectively. As with AVP, magnocellular cells of the PVH and SON served as positive controls while the brain from AVP–knockout mouse served a negative control.

Slides were baked at 60 °C for 1 h, deparaffinized, incubated with hydrogen peroxide for 10 min at room temperature, pretreated with Target Retrieval Reagent (#322001) for 20 min at 100 °C and with Protease III for 30 min at 40 °C. Probe hybridization and signal amplification were performed as per the manufacturer's instructions for chromogenic assays.

Following RNAscope assay, the slides were scanned at ×20 magnification and the digital image analysis was successfully validated using the CaseViewer 2.4 (3DHISTECH) software. The same software was employed to capture and prepare images for the figures in the article. Images of control tissues were taken using microscope Leica DM 1000 LED. Detection of *Avp*- and *Avpr1a*–positive cells was also performed using the QuPath-0.2.3 (University of Edinburgh, UK) software. *The Atlas for the Mouse Brain in Stereotaxic Coordinates* (45) was utilized to identify and manually map every nucleus, sub–nucleus or region using drawing features of the QuPath-0.2.3 software in every tenth brain section. This was followed by exhaustive counting of *Avp* and *Avpr1a* transcripts using a tag feature. *Avp* and *Avpr1a* transcript density was calculated by dividing the absolute numbers by the total area (μm^2, ImageJ) of every nucleus, sub–nucleus or region. Photomicrographs were prepared using Photoshop CS5 (Adobe Systems) only to adjust brightness, contrast and sharpness, to remove artifacts (*i.e.,* obscuring bubbles), and to make composite plates.

Quantitation, Validation and Statistical Analysis

Data were analyzed by Student's *t*-test and two-way analysis of variance (ANOVA) followed by Tukey's multiple comparisons tests using GraphPad Prism 10.2.2 version (La Jolla, CA). Significance was set at $P < 0.05$. *P* values are shown.

ACKNOWLEDGEMENTS

Work at Icahn School of Medicine at Mount Sinai carried at the Center for Translational Medicine and Pharmacology was supported by R01 AG071870 to M.Z., T.Y., and S.-M.K.; R01 AG074092 and U01AG073148 to T.Y. and M.Z.; U19 AG060917 and R01 DK113627 to M.Z.

REFERENCES

1. M. J. Brownstein, J. T. Russell, H. Gainer, Synthesis, transport, and release of posterior pituitary hormones. *Science* **207**, 373-378 (1980).
2. W. S. Young, 3rd, H. Gainer, Transgenesis and the study of expression, cellular targeting and function of oxytocin, vasopressin and their receptors. *Neuroendocrinology* **78**, 185-203 (2003).
3. Y. J. Silva, R. C. Moffat, A. J. Walt, Vasopressin effect on portal and systemic hemodynamics. Studies in intact, unanesthetized humans. *JAMA* **210**, 1065-1068 (1969).
4. J. D. Stockand *et al.*, Chronic activation of vasopressin-2 receptors induces hypertension in Liddle mice by promoting Na(+) and water retention. *Am J Physiol Renal Physiol* **323**, F468-F478 (2022).
5. M. Lukas, I. D. Neumann, Oxytocin and vasopressin in rodent behaviors related to social dysfunctions in autism spectrum disorders. *Behav Brain Res* **251**, 85-94 (2013).
6. M. Lukas, I. Toth, A. H. Veenema, I. D. Neumann, Oxytocin mediates rodent social memory within the lateral septum and the medial amygdala depending on the relevance of the social stimulus: male juvenile versus female adult conspecifics. *Psychoneuroendocrinology* **38**, 916-926 (2013).
7. A. H. Veenema, I. D. Neumann, Central vasopressin and oxytocin release: regulation of complex social behaviours. *Prog Brain Res* **170**, 261-276 (2008).
8. A. Meyer-Lindenberg, G. Domes, P. Kirsch, M. Heinrichs, Oxytocin and vasopressin in the human brain: social neuropeptides for translational medicine. *Nat Rev Neurosci* **12**, 524-538 (2011).
9. H. E. Albers, Species, sex and individual differences in the vasotocin/vasopressin system: relationship to neurochemical signaling in the social behavior neural network. *Front Neuroendocrinol* **36**, 49-71 (2015).
10. J. T. Winslow, N. Hastings, C. S. Carter, C. R. Harbaugh, T. R. Insel, A role for central vasopressin in pair bonding in monogamous prairie voles. *Nature* **365**, 545-548 (1993).
11. T. R. Insel, T. J. Hulihan, A gender-specific mechanism for pair bonding: oxytocin and partner preference formation in monogamous voles. *Behav Neurosci* **109**, 782-789 (1995).
12. R. Dantzer, R. M. Bluthe, G. F. Koob, M. Le Moal, Modulation of social memory in male rats by neurohypophyseal peptides. *Psychopharmacology (Berl)* **91**, 363-368 (1987).
13. N. Rigney, G. J. de Vries, A. Petrulis, Modulation of social behavior by distinct vasopressin sources. *Front Endocrinol (Lausanne)* **14**, 1127792 (2023).
14. R. Landgraf *et al.*, Viral vector-mediated gene transfer of the vole V1a vasopressin receptor in the rat septum: improved social discrimination and active social behaviour. *The European journal of neuroscience* **18**, 403-411 (2003).
15. A. H. Veenema, R. Bredewold, G. J. De Vries, Vasopressin regulates social recognition in juvenile and adult rats of both sexes, but in sex- and age-specific ways. *Horm Behav* **61**, 50-56 (2012).

16. K. M. Dumais, A. H. Veenema, Vasopressin and oxytocin receptor systems in the brain: Sex differences and sex-specific regulation of social behavior. *Front Neuroendocrinol* **40**, 1-23 (2016).
17. J. A. French, J. H. Taylor, A. C. Mustoe, J. Cavanaugh, Neuropeptide diversity and the regulation of social behavior in New World primates. *Front Neuroendocrinol* **42**, 18-39 (2016).
18. S. M. Phelps, M. Okhovat, A. Berrio, Individual Differences in Social Behavior and Cortical Vasopressin Receptor: Genetics, Epigenetics, and Evolution. *Frontiers in neuroscience* **11**, 537 (2017).
19. M. M. Lim *et al.*, Enhanced partner preference in a promiscuous species by manipulating the expression of a single gene. *Nature* **429**, 754-757 (2004).
20. S. Fink, L. Excoffier, G. Heckel, High variability and non-neutral evolution of the mammalian avpr1a gene. *BMC Evol Biol* **7**, 176 (2007).
21. D. Ren, K. R. Chin, J. A. French, Molecular variation in AVP and AVPR1a in New World monkeys (Primates, Platyrrhini): evolution and implications for social monogamy. *PloS one* **9**, e111638 (2014).
22. I. F. Bielsky, S. B. Hu, K. L. Szegda, H. Westphal, L. J. Young, Profound impairment in social recognition and reduction in anxiety-like behavior in vasopressin V1a receptor knockout mice. *Neuropsychopharmacology* **29**, 483-493 (2004).
23. I. D. Neumann, R. Landgraf, Balance of brain oxytocin and vasopressin: implications for anxiety, depression, and social behaviors. *Trends Neurosci* **35**, 649-659 (2012).
24. T. R. Lago *et al.*, The novel vasopressin receptor (V1aR) antagonist SRX246 reduces anxiety in an experimental model in humans: a randomized proof-of-concept study. *Psychopharmacology (Berl)* **238**, 2393-2403 (2021).
25. R. R. Thompson, K. George, J. C. Walton, S. P. Orr, J. Benson, Sex-specific influences of vasopressin on human social communication. *Proc Natl Acad Sci U S A* **103**, 7889-7894 (2006).
26. I. F. Bielsky, S. B. Hu, X. Ren, E. F. Terwilliger, L. J. Young, The V1a vasopressin receptor is necessary and sufficient for normal social recognition: a gene replacement study. *Neuron* **47**, 503-513 (2005).
27. T. R. Insel, Z. X. Wang, C. F. Ferris, Patterns of brain vasopressin receptor distribution associated with social organization in microtine rodents. *J Neurosci* **14**, 5381-5392 (1994).
28. Z. Wang, L. J. Young, Y. Liu, T. R. Insel, Species differences in vasopressin receptor binding are evident early in development: comparative anatomic studies in prairie and montane voles. *J Comp Neurol* **378**, 535-546 (1997).
29. M. M. Lim, L. J. Young, Vasopressin-dependent neural circuits underlying pair bond formation in the monogamous prairie vole. *Neuroscience* **125**, 35-45 (2004).
30. J. Y. Summy-Long, M. Kadekaro, Role of circumventricular organs (CVO) in neuroendocrine responses: interactions of CVO and the magnocellular neuroendocrine system in different reproductive states. *Clin Exp Pharmacol Physiol* **28**, 590-601 (2001).

31. E. M. Stricker, W. Huang, A. F. Sved, Early osmoregulatory signals in the control of water intake and neurohypophyseal hormone secretion. *Physiol Behav* **76**, 415-421 (2002).
32. M. Ludwig, M. F. Callahan, I. Neumann, R. Landgraf, M. Morris, Systemic osmotic stimulation increases vasopressin and oxytocin release within the supraoptic nucleus. *J Neuroendocrinol* **6**, 369-373 (1994).
33. M. Ludwig, G. Leng, Autoinhibition of supraoptic nucleus vasopressin neurons in vivo: a combined retrodialysis/electrophysiological study in rats. *The European journal of neuroscience* **9**, 2532-2540 (1997).
34. B. C. Wang, L. Share, J. T. Crofton, Central infusion of vasopressin decreased plasma vasopressin concentration in dogs. *Am J Physiol* **243**, E365-369 (1982).
35. C. T. Wotjak, M. Ludwig, R. Landgraf, Vasopressin facilitates its own release within the rat supraoptic nucleus in vivo. *Neuroreport* **5**, 1181-1184 (1994).
36. M. Zaidi *et al.*, Actions of pituitary hormones beyond traditional targets. *J Endocrinol* **237**, R83-R98 (2018).
37. C. S. Carter, Oxytocin pathways and the evolution of human behavior. *Annu Rev Psychol* **65**, 17-39 (2014).
38. T. A. Koshimizu *et al.*, Vasopressin V1a and V1b receptors: from molecules to physiological systems. *Physiol Rev* **92**, 1813-1864 (2012).
39. B. Jurek, I. D. Neumann, The Oxytocin Receptor: From Intracellular Signaling to Behavior. *Physiol Rev* **98**, 1805-1908 (2018).
40. R. Tamma *et al.*, Regulation of bone remodeling by vasopressin explains the bone loss in hyponatremia. *Proc Natl Acad Sci U S A* **110**, 18644-18649 (2013).
41. L. Sun *et al.*, Oxytocin regulates body composition. *Proc Natl Acad Sci U S A* 10.1073/pnas.1913611116 (2019).
42. L. Sun *et al.*, Functions of vasopressin and oxytocin in bone mass regulation. *Proc Natl Acad Sci U S A* **113**, 164-169 (2016).
43. R. Tamma *et al.*, Oxytocin is an anabolic bone hormone. *Proc Natl Acad Sci U S A* **106**, 7149-7154 (2009).
44. P. A. Phillips *et al.*, Localization of vasopressin binding sites in rat tissues using specific V1 and V2 selective ligands. *Endocrinology* **126**, 1478-1484 (1990).
45. G. Paxinos, K. B. J. Franklin, *The Mouse Brain in Stereotaxic Coordinates* (Academic Press, New York, ed. 3rd, 2007).
46. G. J. DeVries, R. M. Buijs, D. F. Swaab, Ontogeny of the vasopressinergic neurons of the suprachiasmatic nucleus and their extra-hypothalamic projections in the rat brain-presence of a sex difference in the lateral septum. *Brain Research* **218**, 67-78 (1981).
47. G. J. De Vries, R. M. Buijs, The origin of the vasopressinergic and oxytocinergic innervation of the rat brain with special reference to the lateral septum. *Brain Res* **273**, 307-317 (1983).
48. A. R. Caffe, P. C. Van Ryen, T. P. Van der Woude, F. W. Van Leeuwen, Vasopressin and oxytocin systems in the brain and upper spinal cord of Macaca fascicularis. *J Comp Neurol* **287**, 302-325 (1989).
49. G. J. de Vries, R. M. Buijs, A. A. Sluiter, Gonadal hormone actions on the morphology of the vasopressinergic innervation of the adult rat brain. *Brain Res* **298**, 141-145 (1984).

50. M. A. Miller, G. J. DeVries, H. A. al-Shamma, D. M. Dorsa, Decline of vasopressin immunoreactivity and mRNA levels in the bed nucleus of the stria terminalis following castration. *J Neurosci* **12**, 2881-2887 (1992).
51. G. J. De Vries, H. A. al-Shamma, Sex differences in hormonal responses of vasopressin pathways in the rat brain. *J Neurobiol* **21**, 686-693 (1990).
52. G. J. De Vries, Z. Wang, N. A. Bullock, S. Numan, Sex differences in the effects of testosterone and its metabolites on vasopressin messenger RNA levels in the bed nucleus of the stria terminalis of rats. *J Neurosci* **14**, 1789-1794 (1994).
53. L. Joca, D. G. Zuloaga, J. Raber, J. A. Siegel, Long-term effects of early adolescent methamphetamine exposure on depression-like behavior and the hypothalamic vasopressin system in mice. *Dev Neurosci* **36**, 108-118 (2014).
54. M. Q. Steinman *et al.*, Hypothalamic vasopressin systems are more sensitive to the long term effects of social defeat in males versus females. *Psychoneuroendocrinology* **51**, 122-134 (2015).
55. Z. Wang, Species differences in the vasopressin-immunoreactive pathways in the bed nucleus of the stria terminalis and medial amygdaloid nucleus in prairie voles (Microtus ochrogaster) and meadow voles (Microtus pennsylvanicus). *Behav Neurosci* **109**, 305-311 (1995).
56. Z. Wang, L. Zhou, T. J. Hulihan, T. R. Insel, Immunoreactivity of central vasopressin and oxytocin pathways in microtine rodents: a quantitative comparative study. *J Comp Neurol* **366**, 726-737 (1996).
57. Y. Wang, L. Xu, Y. Pan, Z. Wang, Z. Zhang, Species differences in the immunoreactive expression of oxytocin, vasopressin, tyrosine hydroxylase and estrogen receptor alpha in the brain of Mongolian gerbils (Meriones unguiculatus) and Chinese striped hamsters (Cricetulus barabensis). *PloS one* **8**, e65807 (2013).
58. N. L. Ostrowski *et al.*, Distribution of V1a and V2 vasopressin receptor messenger ribonucleic acids in rat liver, kidney, pituitary and brain. *Endocrinology* **131**, 533-535 (1992).
59. C. L. Zhang *et al.*, Arcuate NPY is involved in salt-induced hypertension via modulation of paraventricular vasopressin and brain-derived neurotrophic factor. *J Cell Physiol* **237**, 2574-2588 (2022).
60. R. Pineda, N. Sabatier, M. Ludwig, R. P. Millar, G. Leng, A Direct Neurokinin B Projection from the Arcuate Nucleus Regulates Magnocellular Vasopressin Cells of the Supraoptic Nucleus. *J Neuroendocrinol* **28** (2016).
61. Y. Maejima *et al.*, Oxytocinergic circuit from paraventricular and supraoptic nuclei to arcuate POMC neurons in hypothalamus. *FEBS Lett* **588**, 4404-4412 (2014).
62. A. H. Meyer, W. Langhans, E. Scharrer, Vasopressin reduces food intake in goats. *Q J Exp Physiol* **74**, 465-473 (1989).
63. W. Langhans, E. Delprete, E. Scharrer, Mechanisms of vasopressin's anorectic effect. *Physiol Behav* **49**, 169-176 (1991).
64. A. Kalsbeek, E. Fliers, M. A. Hofman, D. F. Swaab, R. M. Buijs, Vasopressin and the output of the hypothalamic biological clock. *J Neuroendocrinol* **22**, 362-372 (2010).
65. E. Trudel, C. W. Bourque, Central clock excites vasopressin neurons by waking osmosensory afferents during late sleep. *Nat Neurosci* **13**, 467-474 (2010).

66. C. Gizowski, C. Zaelzer, C. W. Bourque, Clock-driven vasopressin neurotransmission mediates anticipatory thirst prior to sleep. *Nature* **537**, 685-688 (2016).
67. J. Dai, D. F. Swaab, R. M. Buijs, Recovery of axonal transport in "dead neurons". *Lancet* **351**, 499-500 (1998).
68. J. Dai, D. F. Swaab, J. Van der Vliet, R. M. Buijs, Postmortem tracing reveals the organization of hypothalamic projections of the suprachiasmatic nucleus in the human brain. *J Comp Neurol* **400**, 87-102 (1998).
69. K. E. Rohr, A. Telega, A. Savaglio, J. A. Evans, Vasopressin regulates daily rhythms and circadian clock circuits in a manner influenced by sex. *Horm Behav* **127**, 104888 (2021).
70. M. Yoshimura, B. Conway-Campbell, Y. Ueta, Arginine vasopressin: Direct and indirect action on metabolism. *Peptides* **142**, 170555 (2021).
71. L. J. Young, D. Toloczko, T. R. Insel, Localization of vasopressin (V1a) receptor binding and mRNA in the rhesus monkey brain. *J Neuroendocrinol* **11**, 291-297 (1999).
72. E. Szczepanska-Sadowska, A. Wsol, A. Cudnoch-Jedrzejewska, T. Zera, Complementary Role of Oxytocin and Vasopressin in Cardiovascular Regulation. *International journal of molecular sciences* **22** (2021).
73. I. J. Edwards, S. A. Deuchars, J. Deuchars, The intermedius nucleus of the medulla: a potential site for the integration of cervical information and the generation of autonomic responses. *J Chem Neuroanat* **38**, 166-175 (2009).
74. B. S. Zanutto, M. E. Valentinuzzi, E. T. Segura, Neural set point for the control of arterial pressure: role of the nucleus tractus solitarius. *Biomed Eng Online* **9**, 4 (2010).
75. R. F. Baumeister, M. R. Leary, The need to belong: desire for interpersonal attachments as a fundamental human motivation. *Psychol Bull* **117**, 497-529 (1995).
76. U. Wagner *et al.*, Beautiful friendship: Social sharing of emotions improves subjective feelings and activates the neural reward circuitry. *Soc Cogn Affect Neurosci* **10**, 801-808 (2015).
77. N. Rigney, R. Beaumont, A. Petrulis, Sex differences in vasopressin 1a receptor regulation of social communication within the lateral habenula and dorsal raphe of mice. *Horm Behav* **121**, 104715 (2020).
78. B. D. Rood *et al.*, Site of origin of and sex differences in the vasopressin innervation of the mouse (Mus musculus) brain. *J Comp Neurol* **521**, 2321-2358 (2013).
79. V. A. Tobin *et al.*, An intrinsic vasopressin system in the olfactory bulb is involved in social recognition. *Nature* **464**, 413-417 (2010).
80. F. Levy, K. M. Kendrick, J. A. Goode, R. Guevara-Guzman, E. B. Keverne, Oxytocin and vasopressin release in the olfactory bulb of parturient ewes: changes with maternal experience and effects on acetylcholine, gamma-aminobutyric acid, glutamate and noradrenaline release. *Brain Res* **669**, 197-206 (1995).

81. M. D. Reed, K. E. Price, J. Archbold, A. Moffa, M. Febo, Predator odor-evoked BOLD activation in the awake rat: modulation by oxytocin and V(1)a vasopressin receptor antagonists. *Brain Res* **1494**, 70-83 (2013).
82. D. De Wied, Long term effect of vasopressin on the maintenance of a conditioned avoidance response in rats. *Nature* **232**, 58-60 (1971).
83. L. Zhang *et al.*, Vasopressin induces depolarization and state-dependent firing patterns in rat thalamic paraventricular nucleus neurons in vitro. *Am J Physiol Regul Integr Comp Physiol* **290**, R1226-1232 (2006).
84. H. Matsuguchi, F. M. Sharabi, F. J. Gordon, A. K. Johnson, P. G. Schmid, Blood pressure and heart rate responses to microinjection of vasopressin into the nucleus tractus solitarius region of the rat. *Neuropharmacology* **21**, 687-693 (1982).
85. F. M. Faraci, W. G. Mayhan, W. J. Farrell, D. D. Heistad, Humoral regulation of blood flow to choroid plexus: role of arginine vasopressin. *Circ Res* **63**, 373-379 (1988).

FIGURE LEGENDS

Figure 1: Sex–specific *Avp* transcript density in the brain. (**A**) *Avp* transcript density in main brain regions detected by RNAscope. Female 3V region and hypothalamus and male hypothalamus had the highest *Avp* transcript density. (**B**) Representative micrographs of some of the hypothalamic and forebrain regions with highest *Avp* expression. Scale bar: 20 µm. (**C**) *Avp* transcript density in nuclei, sub–nuclei and regions of the hypothalamus and forebrain. (**D**) Novel *Avp* transcripts found in nuclei, sub–nuclei and regions of the hippocampus, thalamus and cerebral cortex. Scale bar: 10 µm. Note, that *Avp* transcripts were found only in the female 3V ependymal layer and thalamus. *N*=3 mice *per* sex.

Figure 2: Sex–specific *Avpr1a* transcript density in the brain. (**A**) Probe specificity was established by a positive signal in renal tubules of the kidney (positive control) with an absent signal in the frontal association cortex (FrA) (negative control). Also shown are representative micrographs of medullary central canal (CC) and hypothalamic arcuate nucleus (Arc). (**B**) *Avpr1a* transcript density in main brain regions detected by RNAscope. (**C**) *Avpr1a* transcript density in nuclei, sub–nuclei and regions of the ventricular regions, hypothalamus, medulla, midbrain and pons, forebrain, olfactory bulb, hippocampus, thalamus, cortex and cerebellum. *N*=3 mice *per* sex. Scale bar: 25 µm (controls) and 20 µm in (A).

Figure 3: *Avp* and *Avpr1a* co-localization in the brain. We found that various nuclei and sub–nuclei exhibited *Avp* and *Avpr1a* co-localization in the brain of both sexes. (**A**)

Female and (**B**) male *Avpr1a* to *Avp* ratios in the cortex, forebrain, hippocampus, 3rd ventricular region, thalamus and hypothalamus.

<u>Figure 4</u>: *Avp* and *Avpr1a* transcript densities in the pituitary gland. RNAscope revealed *Avp* and *Avpr1a* expression in the posterior pituitary lobe with *Avp* and *Avpr1a* transcript densities that were higher in male compared with female mice. . *N*=3 mice *per* sex.

<u>Supplementary Figure 1</u>: Sex–specific *Avp* transcript numbers in the brain. (**A**) Total numbers of *Avp*–positive cells in main brain regions detected by RNAscope. (**B**) Total numbers of *Avp*–positive cells in nuclei, sub–nuclei and regions of the hypothalamus, hippocampus, forebrain and cortex. Note, that *Avp*–positive cells were found only in the female 3V ependymal layer and thalamus. Also shown are representative RNAscope micrographs of hypothalamic regions with highest *Avp* expression; *i.e.*, supraotpic nucleus (SO), paraventricular hypothalamic nucleus, lateral magnocellular part (PaLM), retrochiasmatic area (RCh), supraoptic nucleus, retrochiasmatic part (SOR) and suprachiasmatic nucleus (SCh). . *N*=3 mice *per* sex. Scale bar: 20 µm.

<u>Supplementary Figure 2</u>: Sex–specific *Avpr1a* transcript numbers in the brain. (**A**) Tolal *Avpr1a* transcript numbers in main brain regions detected by RNAscope. (**B**) *Avpr1a* transcript density in nuclei, sub–nuclei and regions of the medulla, hypothalamus, cortex, midbrain and pons, forebrain, thalamus, cerebellum,

hippocampus, olfactory bulb and ventricular regions. Also shown are representative RNAscope micrographs of medullary regions with highest *Avpr1a* expression; *i.e.*, hypoglossal nucleus (12N), intermediate reticular nucleus (IRt), lateral reticular nucleus (LRt) and medullary reticular nucleus, ventral part (MdV). . *N*=3 mice *per* sex. Scale bar: 20 µm.

Appendix: Glossary of the brain nuclei, sub–nuclei and regions.

Figure 1A

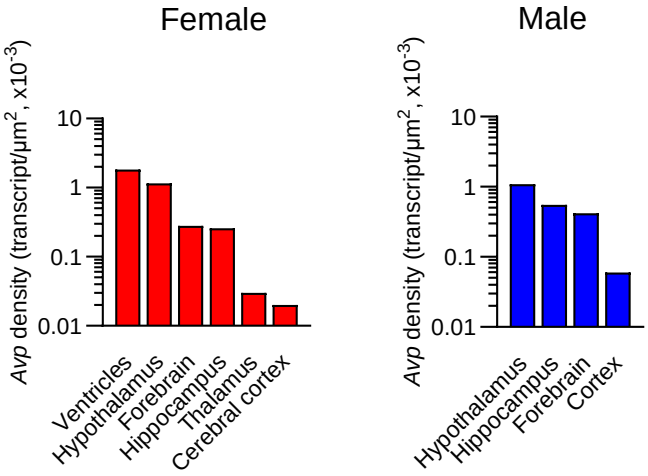
Female
Male
Avp density (transcript/µm2, x10-3)
10
1
0.1
0.01
Ventricles
Hypothalamus
Forebrain
Hippocampus
Thalamus
Cerebral cortex
Hypothalamus
Hippocampus
Forebrain
Cortex

Figure 1B

3V region

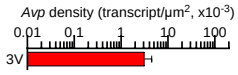

Hypothalamus

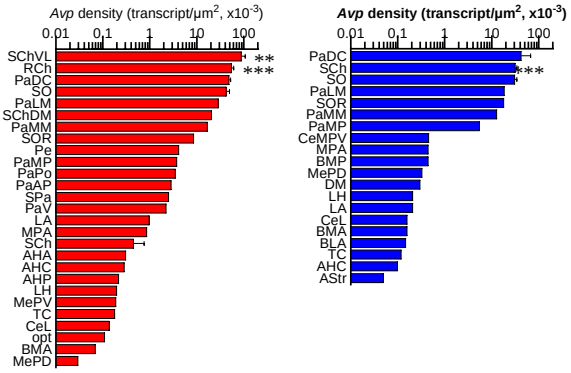

Forebrain

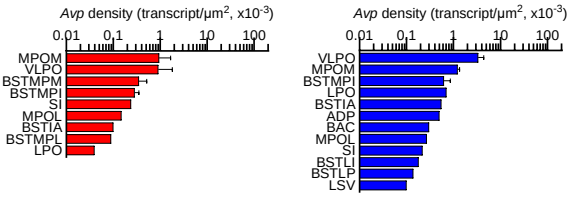

Hippocampus

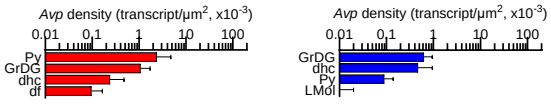

Thalamus

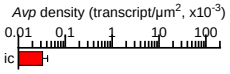

Cortex

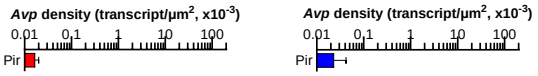

Figure 1C

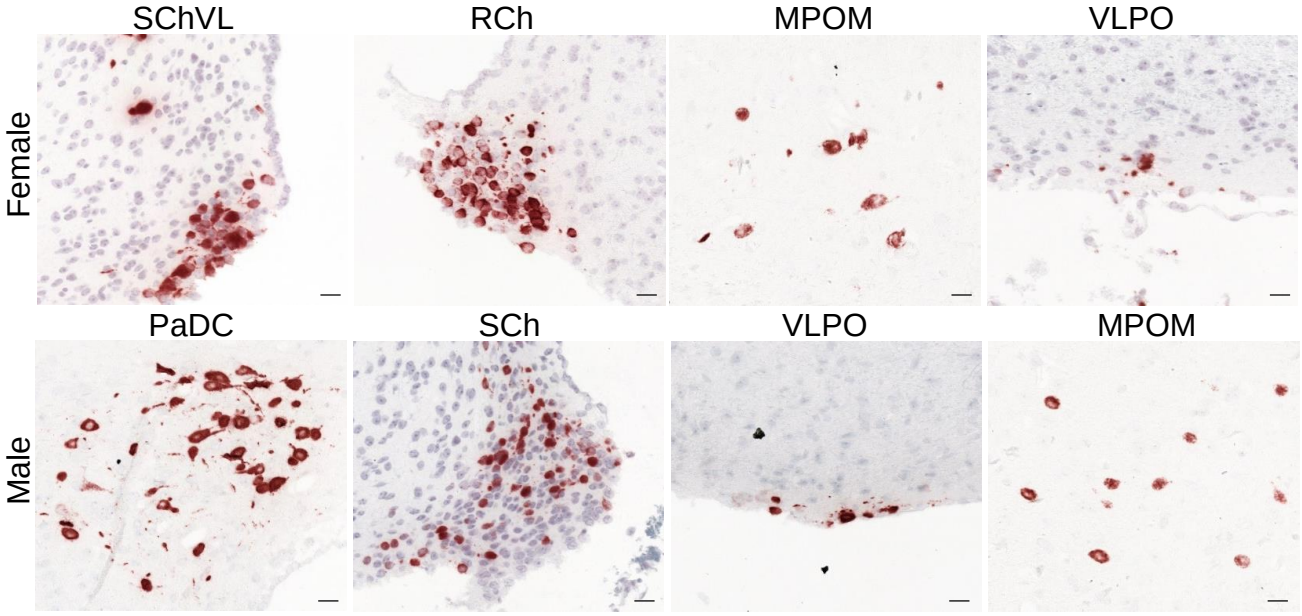

Figure 1D

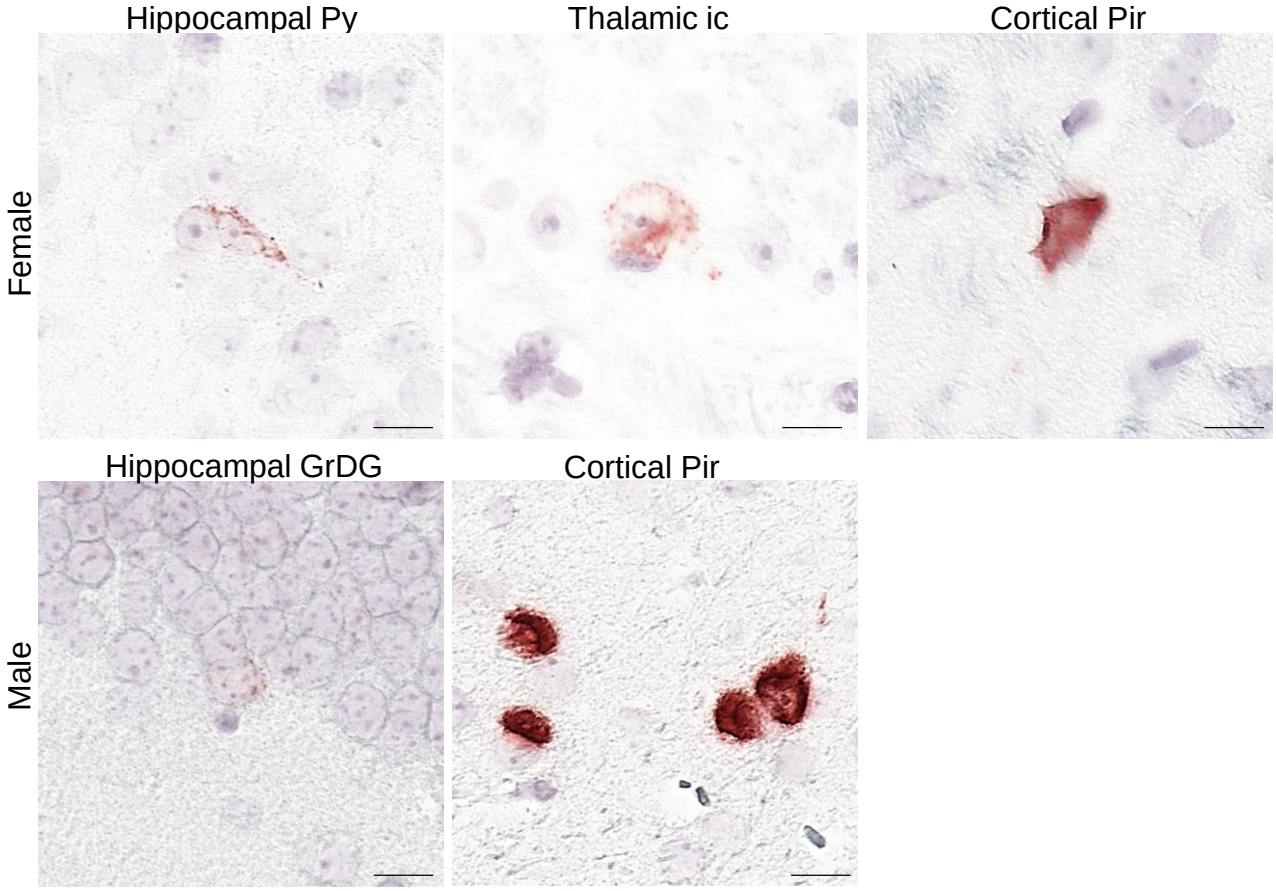
Hippocampal Py
Thalamic ic
Cortical Pir
Female
Hippocampal GrDG
Cortical Pir
Male

Figure 2A

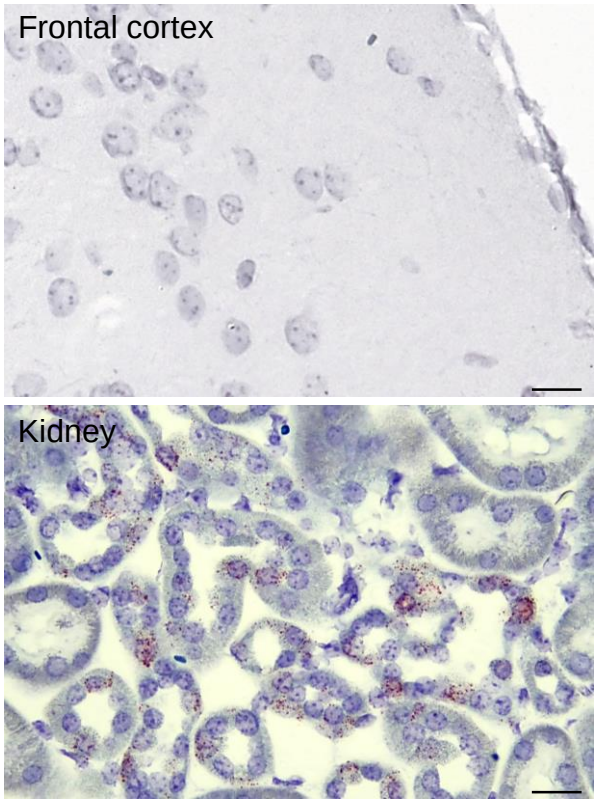

Figure 2A

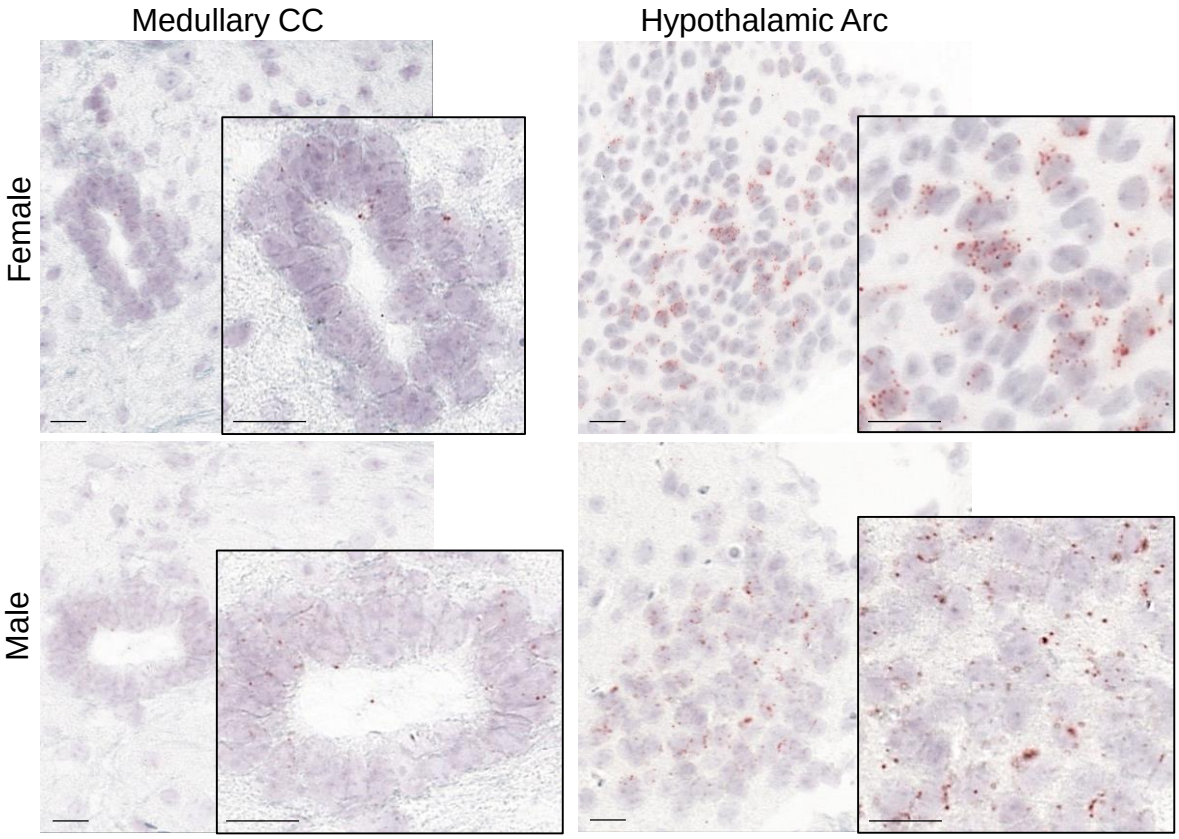

AVPR1a density in brain divisions

Figure 2B

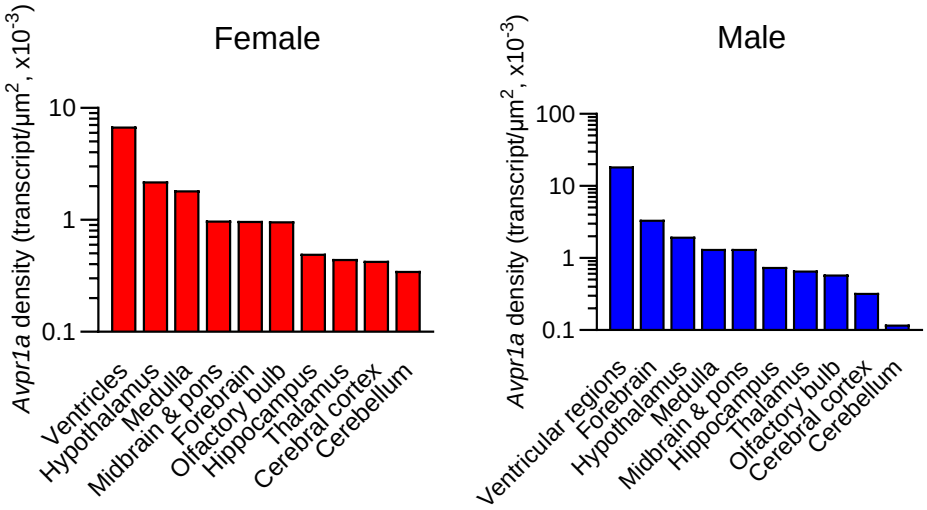

Figure 2C

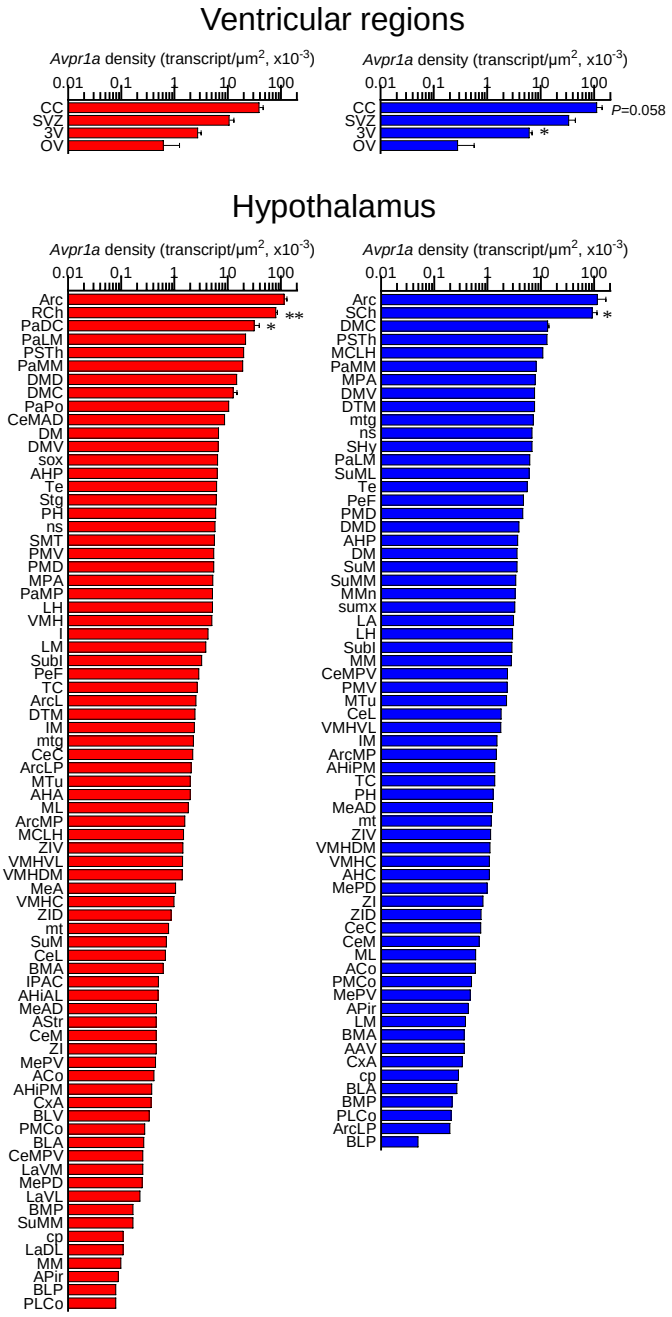
Ventricular regions
Avpr1a density (transcript/μm2, x10-3)
0.01 0.1 1 10 100
CC
SVZ
3V
OV
P=0.058
*
Hypothalamus
Avpr1a density (transcript/μm2, x10-3)
0.01 0.1 1 10 100
Arc
RCh
PaDC
PaLM
PSTh
PaMM
DMD
DMC
PaPo
CeMAD
DM
DMV
sox
AHP
Te
Stg
PH
ns
SMT
PMV
PMD
MPA
PaMP
LH
VMH
I
LM
SubI
PeF
TC
ArcL
DTM
IM
mtg
CeC
ArcLP
MTu
AHA
ML
ArcMP
MCLH
ZIV
VMHVL
VMHDM
MeA
VMHC
ZID
mt
SuM
CeL
BMA
IPAC
AHiAL
MeAD
AStr
CeM
ZI
MePV
ACo
AHiPM
CxA
BLV
PMCo
BLA
CeMPV
LaVM
MePD
LaVL
BMP
SuMM
cp
LaDL
MM
APir
BLP
PLCo
**
*
SCh
DMC
PSTh
MCLH
PaMM
MPA
DMV
DTM
mtg
ns
SHy
PaLM
SuML
Te
PeF
PMD
DMD
AHP
DM
SuM
SuMM
MMn
sumx
LA
LH
SubI
MM
CeMPV
PMV
MTu
CeL
VMHVL
IM
ArcMP
AHiPM
TC
PH
MeAD
mt
ZIV
VMHDM
VMHC
AHC
MePD
ZI
ZID
CeC
CeM
ML
ACo
PMCo
MePV
APir
LM
BMA
AAV
CxA
cp
BLA
BMP
PLCo
ArcLP
BLP

Figure 2C

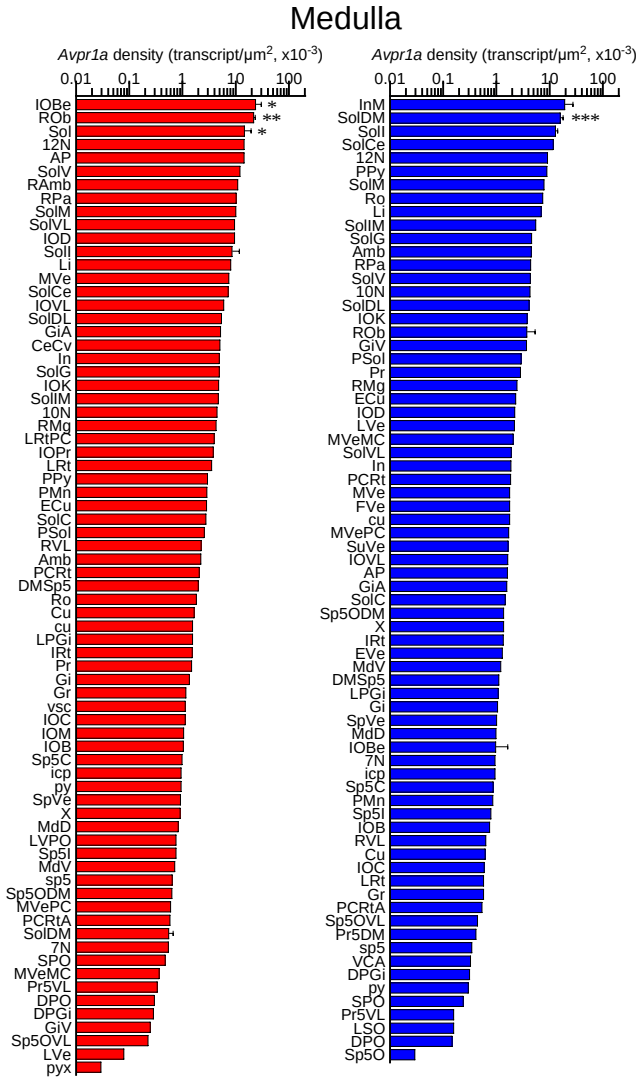
Medulla
Avpr1a density (transcript/μm2, x10-3)
0.01
0.1
1
10
100
IOBe
ROb
Sol
12N
AP
SolV
RAmb
RPa
SolM
SolVL
IOD
SolI
Li
MVe
SolCe
IOVL
SolDL
GiA
CeCv
In
SolG
IOK
SolIM
10N
RMg
LRtPC
IOPr
LRt
PPy
PMn
ECu
SolC
PSol
RVL
Amb
PCRt
DMSp5
Ro
Cu
cu
LPGi
IRt
Pr
Gi
Gr
vsc
IOC
IOM
IOB
Sp5C
icp
py
SpVe
X
MdD
LVPO
Sp5I
MdV
sp5
Sp5ODM
MVePC
PCRtA
SolDM
7N
SPO
MVeMC
Pr5VL
DPO
DPGi
GiV
Sp5OVL
LVe
pyx
Avpr1a density (transcript/μm2, x10-3)
0.01
0.1
1
10
100
InM
SolDM
SolI
SolCe
12N
PPy
SolM
Ro
Li
SolIM
SolG
Amb
RPa
SolV
10N
SolDL
IOK
ROb
GiV
PSol
Pr
RMg
ECu
IOD
LVe
MVeMC
SolVL
In
PCRt
MVe
FVe
cu
MVePC
SuVe
IOVL
AP
GiA
SolC
Sp5ODM
X
IRt
EVe
MdV
DMSp5
LPGi
Gi
SpVe
MdD
IOBe
7N
icp
Sp5C
PMn
Sp5I
IOB
RVL
Cu
IOC
LRt
Gr
PCRtA
Sp5OVL
Pr5DM
sp5
VCA
DPGi
py
SPO
Pr5VL
LSO
DPO
Sp5O

Figure 2C

Midbrain & pons

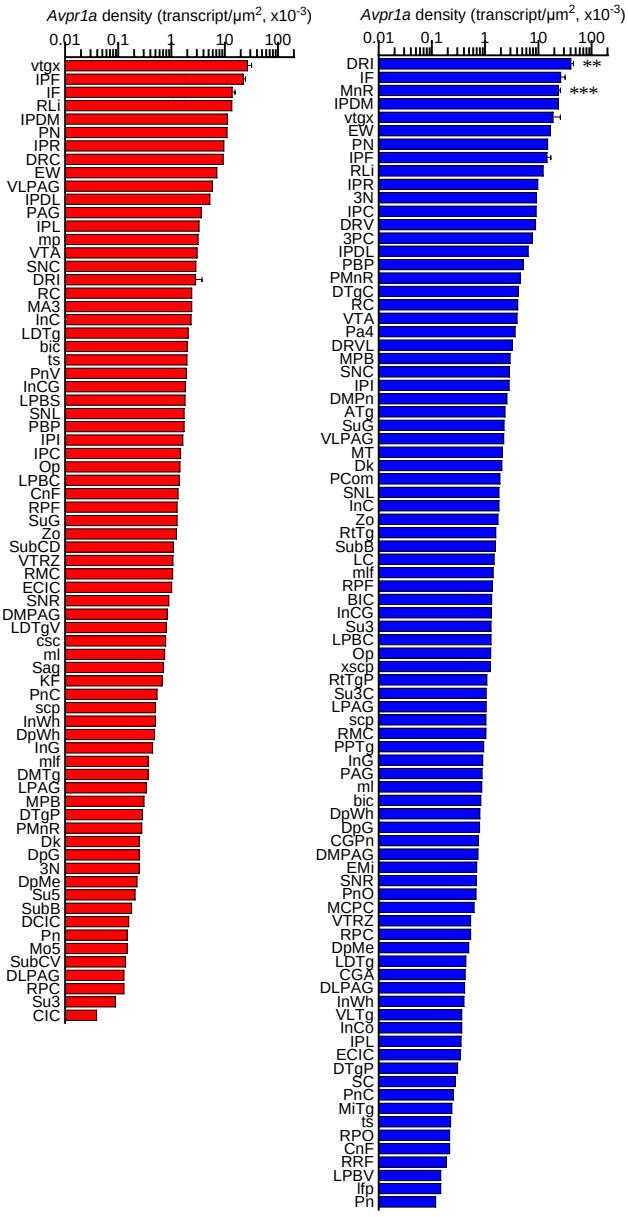

Figure 2C

Forebrain

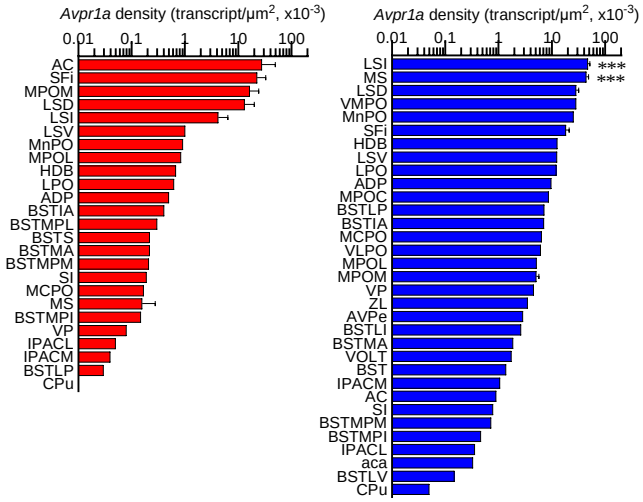

Olfactory bulb

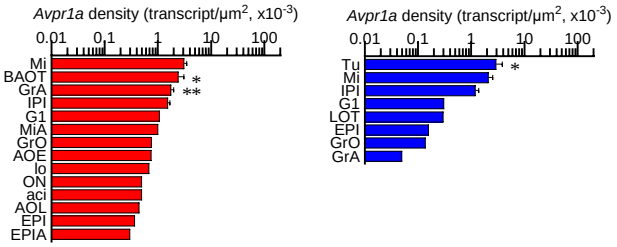

Hippocampus

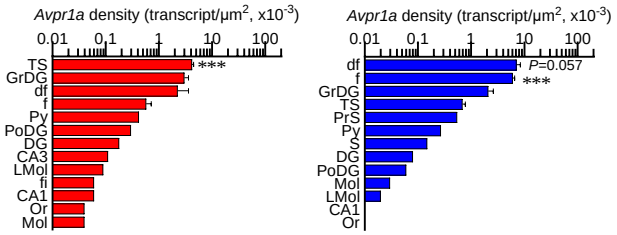

Figure 2C

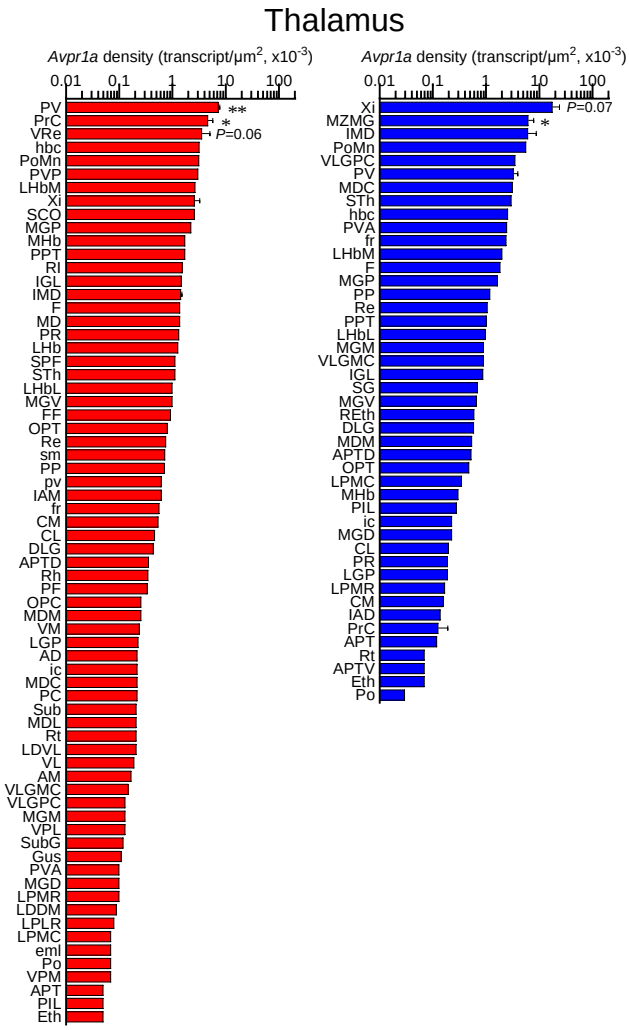
Thalamus
Avpr1a density (transcript/μm2, x10-3)
0.01
0.1
1
10
100
PV
PrC
VRe
hbc
PoMn
PVP
LHbM
Xi
SCO
MGP
MHb
PPT
RI
IGL
IMD
F
MD
PR
LHb
SPF
STh
LHbL
MGV
FF
OPT
Re
sm
PP
pv
IAM
fr
CM
CL
DLG
APTD
Rh
PF
OPC
MDM
VM
LGP
AD
ic
MDC
PC
Sub
MDL
Rt
LDVL
VL
AM
VLGMC
VLGPC
MGM
VPL
SubG
Gus
PVA
MGD
LPMR
LDDM
LPLR
LPMC
eml
Po
VPM
APT
PIL
Eth
**
*
P=0.06
Avpr1a density (transcript/μm2, x10-3)
0.01
0.1
1
10
100
Xi
MZMG
IMD
PoMn
VLGPC
PV
MDC
STh
hbc
PVA
fr
LHbM
F
MGP
PP
Re
PPT
LHbL
MGM
VLGMC
IGL
SG
MGV
REth
DLG
MDM
APTD
OPT
LPMC
MHb
PIL
ic
MGD
CL
PR
LGP
LPMR
CM
IAD
PrC
APT
Rt
APTV
Eth
Po
P=0.07
*

Figure 2C

Cortex

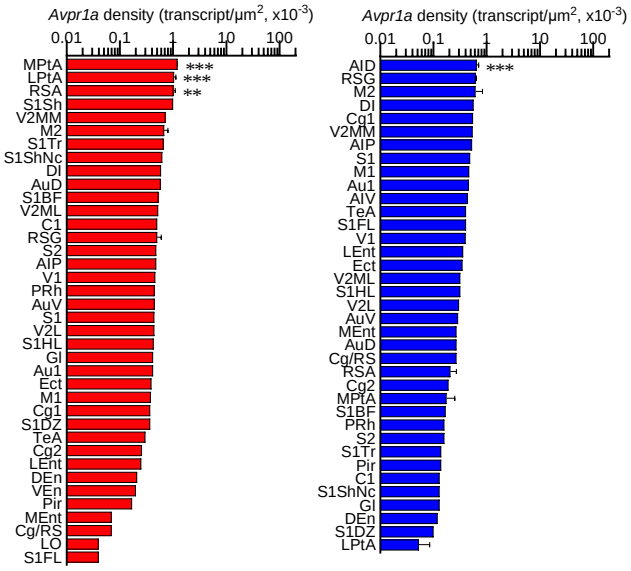

Cerebellum

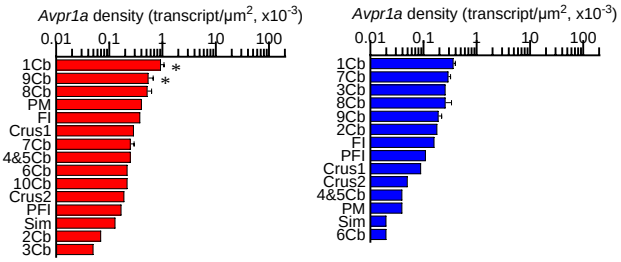

Figure 3A

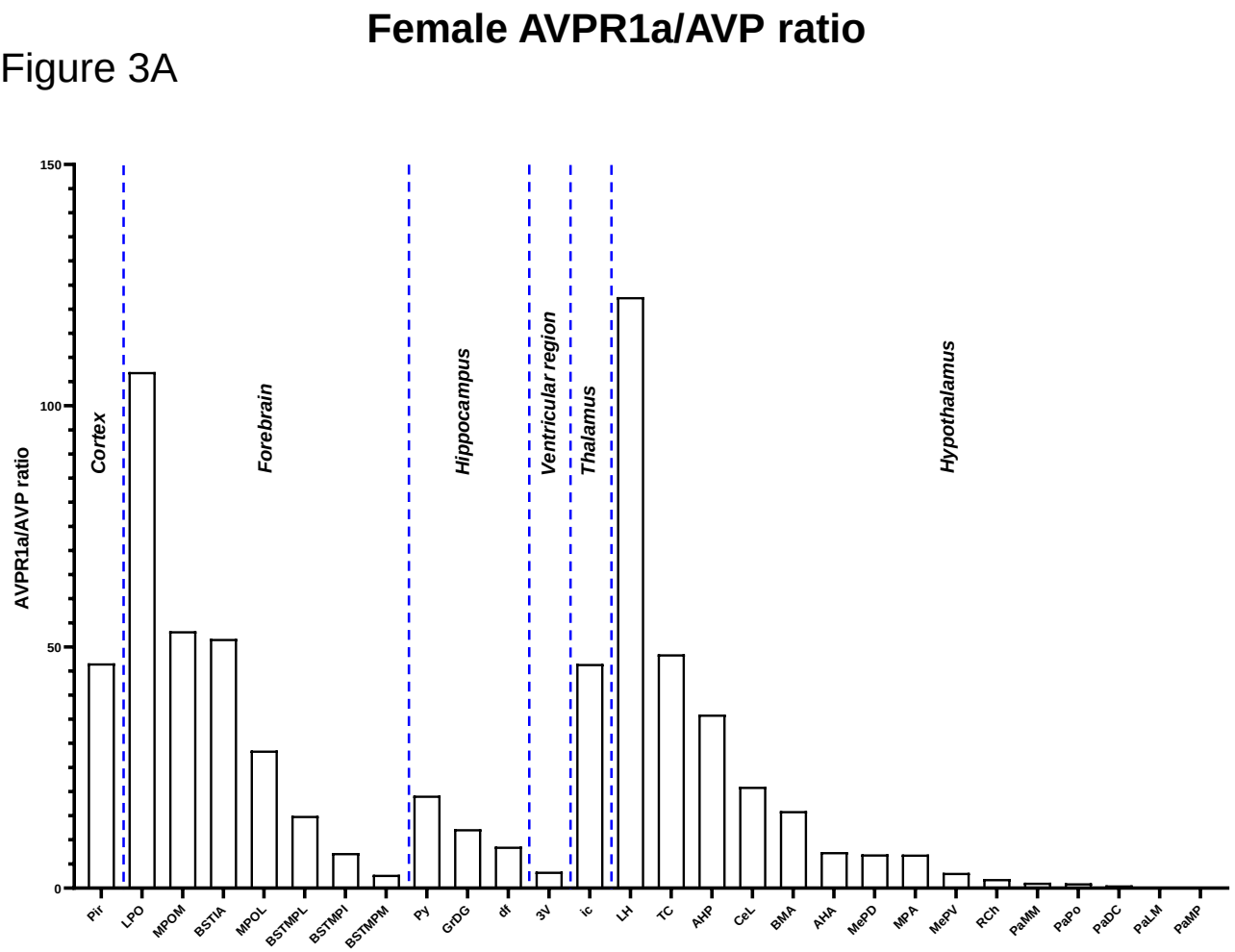
Female AVPR1a/AVP ratio
AVPR1a/AVP ratio
150
100
50
0
Cortex
Forebrain
Hippocampus
Ventricular region
Thalamus
Hypothalamus
Pir
LPO
MPOM
BSTIA
MPOL
BSTMPL
BSTMPI
BSTMPM
Py
GrDG
df
3V
ic
LH
TC
AHP
CeL
BMA
AHA
MePD
MPA
MePV
RCh
PaMM
PaPo
PaDC
PaLM
PaMP

Figure 3B

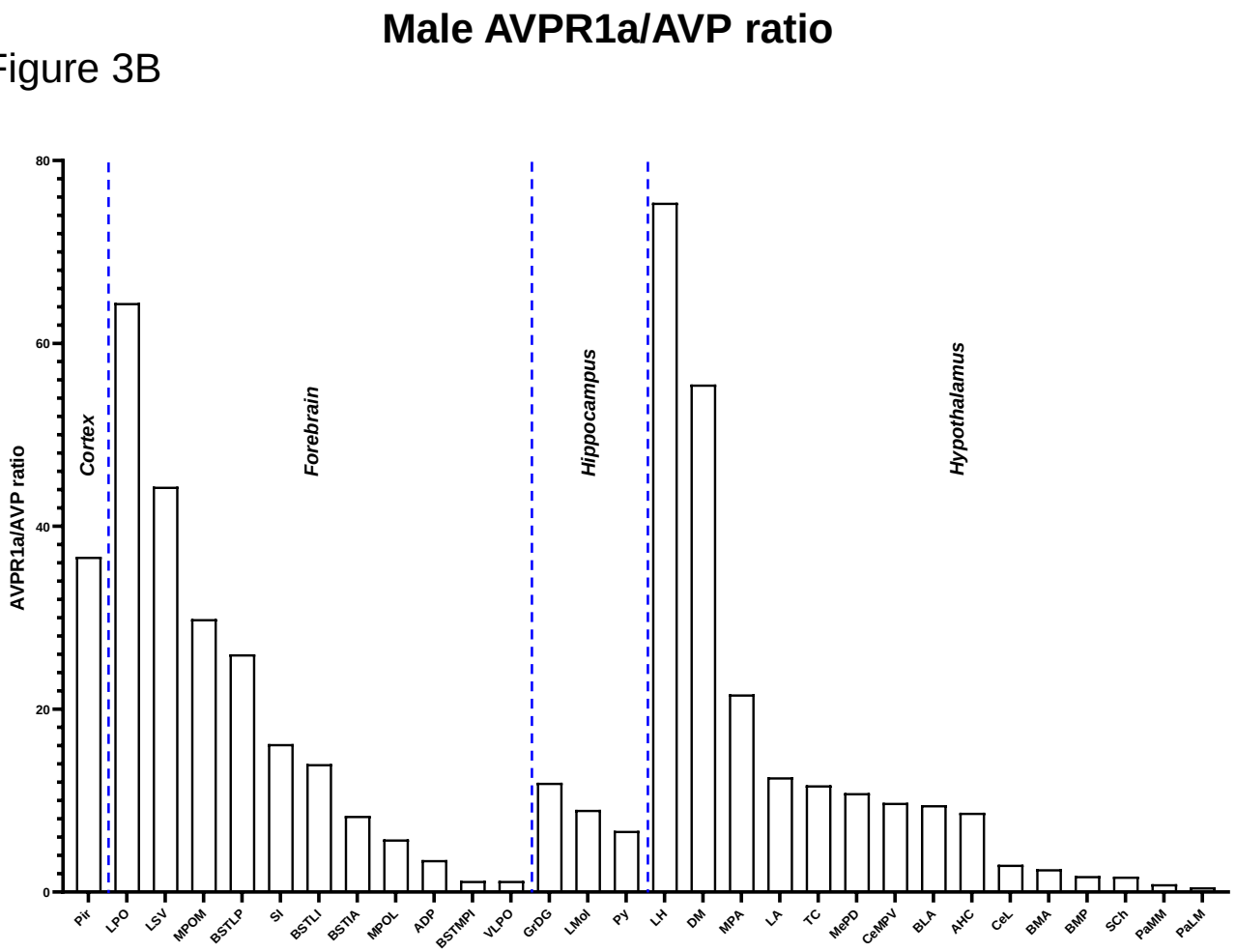
Male AVPR1a/AVP ratio
AVPR1a/AVP ratio
80
60
40
20
0
Cortex
Forebrain
Hippocampus
Hypothalamus
Pir
LPO
LSV
MPOM
BSTLP
SI
BSTLI
BSTIA
MPOL
ADP
BSTMPI
VLPO
GrDG
LMol
Py
LH
DM
MPA
LA
TC
MePD
CeMPV
BLA
AHC
CeL
BMA
BMP
SCh
PaMM
PaLM

Figure 4

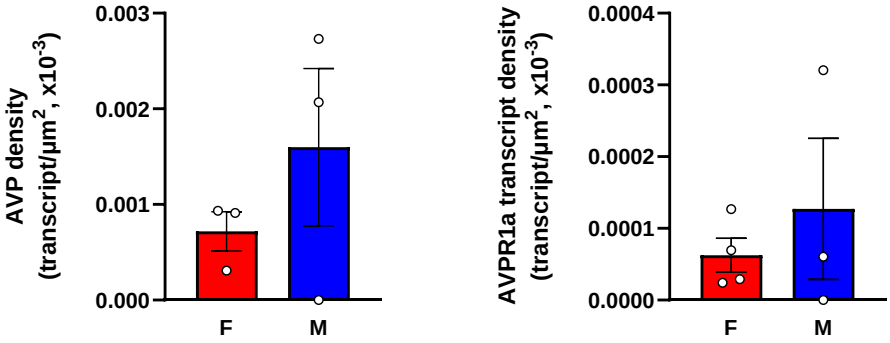
AVP density
(transcript/µm^2, x10^{-3})
0.003
0.002
0.001
0.000
F
M
AVPR1a transcript density
(transcript/µm^2, x10^{-3})
0.0004
0.0003
0.0002
0.0001
0.0000
F
M

Olfactory bulb

aci	anterior commissure, intrabulbar part
AOE	anterior olfactory nucleus, external part
AOL	anterior olfactory nucleus, lateral part
BAOT	bed nucleus of the accessory olfactory tract
EPI	external plexiform layer of the olfactory bulb
EPIA	external plexiform layer of the accessory olfactory bulb
G1	glomerular layer of the olfactory bulb
GrA	granule cell layer of the accessory olfactory bulb
GrO	granular cell layer of the olfactory bulb
IPI	interpeduncular nucleus, intermediate subnucleus
lo	lateral olfactory tract
LOT	nucleus of the lateral olfactory tract
Mi	mitral cell layer of the olfactory bulb
MiA	mitral cell layer of the accessory olfactory bulb
ON	olfactory nerve layer
Tu	olfactory tubercle

Cerebral cortex

AID	agranular insular cortex, dorsal part
AIP	agranular insular cortex, posterior part
AIV	agranular insular cortex, ventral part
Au1	primary auditory cortex
AuD	secondary auditory cortex, dorsal area
AuV	secondary auditory cortex, ventral area
Cg/RS	cingular/retrosplenial cortex
Cg1	cingulate cortex, area 1
Cg2	cingulate cortex, area 2
C1	C1 adrenaline cells
DEn	dorsal endopiriform nucleus
DI	dysgranular insular cortex
Ect	ectorhinal cortex
GI	granular insular cortex
LEnt	lateral entorhinal cortex
LO	lateral orbital cortex
LPtA	lateral parietal association cortex
M1	primary motor cortex
M2	secondary motor cortex
MEnt	medial entorhinal cortex
MPtA	medial parietal association cortex
Pir	piriform cortex
PRh	perirhinal cortex
RSA	retrosplenial agranular cortex
RSG	retrosplenial granular cortex
S1	primary somatosensory cortex
S1BF	primary somatosensory cortex, barrel field
S1DZ	primary somatosensory cortex, dysgranular region
S1FL	primary somatosensory cortex, forelimb region
S1HL	primary somatosensory cortex, hindlimb region
S1Sh	primary somatosensory cortex, shoulder region
S1ShNc	primary somatosensory cortex, shoulder/neck region
S1Tr	primary somatosensory cortex, trunk region

S2	secondary somatosensory cortex
TeA	temporal association cortex
V1	primary visual cortex
V2L	secondary visual cortex, lateral area
V2ML	secondary visual cortex, mediolateral area
V2MM	secondary visual cortex, mediomedial area
VEn	ventral endopiriform nucleus
Forebrain	
AC	anterior commissural nucleus
aca	anterior commissure, anterior part
ADP	anterodorsal preoptic nucleus
AVPe	anteroventral periventricular nucleus
BAC	bed nucleus of the anterior commissure
BST	bed nucleus of the stria terminalis
BSTIA	bed nucleus of the stria terminalis, intraamygdaloid division
BSTLI	bed nucleus of the stria terminalis, lateral division, intermediate part
BSTLP	bed nucleus of the stria terminalis, lateral division, posterior part
BSTLV	bed nucleus of the stria terminalis, lateral division, ventral part
BSTMA	bed nucleus of the stria terminalis, medial division, anterior part
BSTMPI	bed nucleus of the stria terminalis, medial division, posterointermediate part
BSTMPL	bed nucleus of the stria terminalis, medial division, posterolateral part
BSTMPM	bed nucleus of the stria terminalis, medial division, posteromedial part
BSTS	bed nucleus of stria terminalis, supracapsular part
CPu	caudate putamen (striatum)
HDB	nucleus of the horizontal limb of the diagonal band
IPACL	interstitial nucleus of the posterior limb of the anterior commissure, lateral part
IPACM	interstitial nucleus of the posterior limb of the anterior commissure, medial part
LPO	lateral preoptic area
LSD	lateral septal nucleus, dorsal part
LSI	lateral septal nucleus, intermediate part
LSV	lateral septal nucleus, ventral part
MCPO	magnocellular preoptic nucleus
MnPO	median preoptic nucleus
MPOC	medial preoptic nucleus, central part
MPOL	medial preoptic nucleus, lateral part
MPOM	medial preoptic nucleus, medial part
MS	medial septal nucleus
SFi	septofimbrial nucleus
SI	substantia innominata
VLPO	ventrolateral preoptic nucleus
VMPO	ventromedial preoptic nucleus
VOLT	vascular organ of the lamina terminalis
VP	ventral pallidum
ZL	zona limitans
Hippocampus	
CA1	field ca1 of hippocampus
CA3	field CA3 of hippocampus
df	dorsal fornix
DG	dentate gyrus

dhc	dorsal hippocampal commissure
f	fornix
fi	fimbria of the hippocampus
GrDG	granular layer of the dentate gyrus
LMol	lacunosum moleculare layer of the hippocampus
Mol	molecular layer of the dentate gyrus
Or	oriens layer of the hippocampus
PoDG	polymorph layer of the dentate gyrus
PrS	presubiculum
Py	pyramidal tract
S	subiculum
TS	triangular septal nucleus
Thalamus	
AD	anterodorsal thalamic nucleus
AM	anteromedial thalamic nucleus
APT	anterior pretectal nucleus
APTD	anterior pretectal nucleus, dorsal part
APTV	anterior pretectal nucleus, ventral part
CL	centrolateral thalamic nucleus
CM	central medial thalamic nucleus
DLG	dorsal lateral geniculate nucleus
eml	external medullary lamina
Eth	ethmoid thalamic nucleus
F	nucleus of the fields of Forel
FF	fields of Forel
fr	fasciculus retroflexus
Gus	gustatory thalamic nucleus
hbc	habenular commissure
IAD	interanterodorsal thalamic nucleus
IAM	interanteromedial thalamic nucleus
ic	internal capsule
IGL	intergeniculate leaf
IMD	intermediodorsal thalamic nucleus
LDDM	laterodorsal thalamic nucleus, dorsomedial part
LDVL	laterodorsal thalamic nucleus, ventrolateral part
LGP	lateral globus pallidus
LHb	lateral habenular nucleus
LHbL	lateral habenular nucleus, lateral part
LHbM	lateral habenular nucleus, medial part
LPLR	lateral posterior thalamic nucleus, laterorostral part
LPMC	lateral posterior thalamic nucleus, mediocaudal part
LPMR	lateral posterior thalamic nucleus, mediorostral part
MD	mediodorsal thalamic nucleus
MDC	mediodorsal thalamic nucleus, central part
MDL	mediodorsal thalamic nucleus, lateral part
MDM	mediodorsal thalamic nucleus, medial part
MGD	medial geniculate nucleus, dorsal part
MGM	medial geniculate nucleus, medial part
MGP	medial globus pallidus (entopeduncular nucleus)
MGV	medial geniculate nucleus, ventral part
MHb	medial habenular nucleus

MZMG	marginal zone of the medial geniculate
OPC	oval paracentral thalamic nucleus
OPT	olivary pretectal nucleus
PC	paracentral thalamic nucleus
PF	parafascicular thalamic nucleus
PIL	posterior intralaminar thalamic nucleus
Po	posterior thalamic nuclear group
PoMn	posteromedian thalamic nucleus
PP	peripeduncular nucleus
PPT	posterior pretectal nucleus
PR	prerubral field
PrC	precommissural nucleus
pv	periventricular fiber system
PV	paraventricular thalamic nucleus
PVA	paraventricular thalamic nucleus, anterior part
PVP	paraventricular thalamic nucleus, posterior part
Re	reuniens thalamic nucleus
REth	retroethmoid nucleus
Rh	rhomboid thalamic nucleus
RI	rostral interstitial nucleus of medial longitudinal fasciculus
Rt	reticular thalamic nucleus
SCO	subcommissural organ
SG	supragenicular thalamic nucleus
sm	stria medullaris of the thalamus
SPF	subparafascicular thalamic nucleus
STh	subthalamic nucleus
Sub	submedius thalamic nucleus
SubG	subgeniculate nucleus
VL	ventrolateral thalamic nucleus
VLGMC	ventral lateral geniculate nucleus, magnocellular part
VLGPC	ventral lateral geniculate nucleus, parvicellular part
VM	ventromedial thalamic nucleus
VPL	ventral posterolateral thalamic nucleus
VPM	ventral posteromedial thalamic nucleus
VRe	ventral reuniens thalamic nucleus
Xi	xiphoid thalamic nucleus
Hypothalamus	
AAV	anterior amygdaloid area, ventral part
ACo	anterior cortical amygdaloid nucleus
AHA	anterior hypothalamic area, anterior part
AHC	anterior hypothalamic area, central part
AHiAL	amygdalohippocampal area, anterolateral part
AHiPM	amygdalohippocampal area, posteromedial part
AHP	anterior hypothalamic area, posterior part
APir	amygdalopiriform transition area
Arc	arcuate hypothalamic nucleus
ArcL	arcuate hypothalamic nucleus, lateral part
ArcLP	arcuate hypothalamic nucleus, lateroposterior part
ArcMP	arcuate hypothalamic nucleus, medial posterior part
AStr	amygdalostriatal transition area
BLA	basolateral amygdaloid nucleus, anterior part

BLP	basolateral amygdaloid nucleus, posterior part
BLV	basolateral amygdaloid nucleus, ventral part
BMA	basolateral amygdaloid nucleus, anterior part
BMP	basomedial amygdaloid nucleus, posterior part
CeC	central amygdaloid nucleus, capsular part
CeL	central amygdaloid nucleus, lateral division
CeM	central amygdaloid nucleus, medial division
CeMAD	central amygdaloid nucleus, medial division, anterodorsal part
CeMPV	central amygdaloid nucleus, medial posteroventral part
cp	cerebral peduncle, basal part
CxA	cortex-amygdala transition zone
DM	dorsomedial hypothalamic nucleus
DMC	dorsomedial hypothalamic nucleus, compact part
DMD	dorsomedial hypothalamic nucleus, dorsal part
DMV	dorsomedial hypothalamic nucleus, ventral part
DTM	dorsal tuberomammillary nucleus
I	intercalated nuclei of the amygdala
IM	intercalated amygdaloid nucleus, main part
IPAC	interstitial nucleus of the posterior limb of the anterior commissure
LA	lateroanterior hypothalamic nucleus
LaDL	lateral amygdaloid nucleus, dorsolateral part
LaVL	lateral amygdaloid nucleus, ventrolateral part
LaVM	lateral amygdaloid nucleus, ventromedial part
LH	lateral hypothalamic area
LM	lateral mammillary nucleus
MCLH	magnocellular nucleus of the lateral hypothalamus
MeA	medial amygdaloid nucleus, anterior part
MeAD	medial amygdaloid nucleus, anteriodorsal part
MePD	medial amygdaloid nucleus, posterodorsal part
MePV	medial amygdaloid nucleus, posteroventral part
ML	medial mammillary nucleus, lateral part
MM	medial mammillary nucleus, medial part
MMn	medial mammillary nucleus, median part
MPA	medial preoptic area
mt	mammillothalamic tract
mtg	mammillotegmental tract
MTu	medial tuberal nucleus
ns	nigrostriatal bundle
opt	optic tract
PaAP	paraventricular hypothalamic nucleus, anterior parvicellular part
PaDC	paraventricular hypothalamic nucleus, dorsal cap
PaLM	paraventricular hypothalamic nucleus, lateral magnocellular part
PaMM	paraventricular hypothalamic nucleus, medial magnocellular part
PaMP	paraventricular hypothalamic nucleus, medial parvicellular part
PaPo	paraventricular hypothalamic nucleus, posterior part
PaV	paraventricular hypothalamic nucleus, ventral part
Pe	periventricular hypothalamic nucleus
PeF	perifornical nucleus
PH	posterior hypothalamic area
PLCo	posterolateral cortical amygdaloid nucleus
PMCo	posteromedial cortical amygdaloid nucleus (C3)

PMD	premammillary nucleus, dorsal part
PMV	premammillary nucleus, ventral part
PSTh	parasubthalamic nucleus
RCh	retrochiasmatic area
SCh	suprachiasmatic nucleus
SChDM	suprachiasmatic nucleus, dorsomedial part
SChVL	suprachiasmatic nucleus, ventrolateral part
SHy	septohypothalamic nucleus
SMT	submammillothalamic nucleus
SO	supraoptic nucleus
SOR	supraoptic nucleus, retrochiasmatic part
sox	supraoptic decussation
SPa	subparaventricular zone of the hypothalamus
Stg	stigmoid hypothalamic nucleus
Subl	subincertal nucleus
SuM	supramammillary nucleus
SuML	supramammillary nucleus, lateral part
SuMM	supramammillary nucleus, medial part
sumx	supramammillary decussation
TC	tuber cinereum area
Te	terete hypothalamic nucleus
VMH	ventromedial hypothalamic nucleus
VMHC	ventromedial hypothalamic nucleus, central part
VMHDM	ventromedial hypothalamic nucleus, dorsomedial part
VMHVL	ventromedial hypothalamic nucleus, ventrolateral part
ZI	zona incerta
ZID	zona incerta, dorsal part
ZIV	zona incerta, ventral part
Midbrain and pons	
3N	oculomotor nucleus
3PC	oculomotor nucleus, parvicellular part
ATg	anterior tegmental nucleus
bic	brachium of the inferior colliculus
BIC	nucleus of the brachium of the inferior colliculus
CGA	central gray, alpha part
CGPn	central gray of the pons
CIC	central nucleus of the inferior colliculus
CnF	cuneiform nucleus
csc	commissure of the superior colliculus
DCIC	dorsal cortex of the inferior colliculus
Dk	nucleus of Darkschewitsch
DLPAG	dorsolateral periaqueductal gray
DMPAG	dorsomedial periaqueductal gray
DMPn	dorsomedial pontine nucleus
DMTg	dorsomedial tegmental area
DpG	deep gray layer of the superior colliculus
DpMe	deep mesencephalic nucleus
DpWh	deep white layer of the superior colliculus
DRC	dorsal raphe nucleus, caudal part
DRI	dorsal raphe nucleus, interfascicular part
DRV	dorsal raphe nucleus, ventral part

DRVL	dorsal raphe nucleus, ventrolateral part
DTgC	dorsal tegmental nucleus, central part
DTgP	dorsal tegmental nucleus, pericentral part
ECIC	external cortex of the inferior colliculus
EMi	epimicrocellular nucleus
EW	Edinger-Westphal nucleus
IF	interfascicular nucleus
InC	interstitial nucleus of Cajal
InCG	interstitial nucleus of Cajal, greater part
InCo	intercollicular nucleus
InG	intermediate gray layer of the superior colliculus
InWh	intermediate white layer of the superior colliculus
IPC	interpeduncular nucleus, caudal subnucleus
IPDL	interpeduncular nucleus, dorsolateral subnucleus
IPDM	interpeduncular nucleus, dorsomedial subnucleus
IPF	interpeduncular fossa
IPI	interpeduncular nucleus, intermediate subnucleus
IPL	interpeduncular nucleus, lateral subnucleus
IPR	interpeduncular nucleus, rostral subnucleus
KF	Ko¨lliker-Fuse nucleus
LC	locus coeruleus
LDTg	laterodorsal tegmental nucleus
LDTgV	laterodorsal tegmental nucleus, ventral part
lfp	longitudinal fasciculus of the pons
LPAG	lateral periaqueductal gray
LPBC	lateral parabrachial nucleus, central part
LPBS	lateral parabrachial nucleus, superior part
LPBV	lateral parabrachial nucleus, ventral part
MA3	medial accessory oculomotor nucleus
MCPC	magnocellular nucleus of the posterior commissure
MiTg	microcellular tegmental nucleus
ml	medial lemniscus
mlf	medial longitudinal fasciculus
MnR	median raphe nucleus
Mo5	motor trigeminal nucleus
mp	mammillary peduncle
MPB	medial parabrachial nucleus
MT	medial terminal nucleus of the accessory optic tract
Op	optic nerve layer of the superior colliculus
Pa4	paratrochlear nucleus
PAG	periaqueductal gray
PBP	parabrachial pigmented nucleus
PCom	nucleus of the posterior commissure
PMnR	paramedian raphe nucleus
Pn	pontine nuclei
PN	paranigral nucleus
PnC	pontine reticular nucleus, caudal part
PnO	pontine reticular nucleus, oral part
PnV	pontine reticular nucleus, ventral part
PPTg	pedunculopontine tegmental nucleus
RC	raphe cap

RLi	rostral linear nucleus of the raphe
RMC	red nucleus, magnocellular part
RPC	red nucleus, parvicellular part
RPF	retroparafascicular nucleus
RPO	rostral periolivary region
RRF	retrorubral field
RtTg	reticulotegmental nucleus of the pons
RtTgP	reticulotegmental nucleus of the pons, pericentral part
Sag	sagulum nucleus
SC	superior colliculus
scp	superior cerebellar peduncle (brachium conjunctivum)
SNC	substantia nigra, compact part
SNL	substantia nigra, lateral part
SNR	substantia nigra, reticular part
Su3	supraoculomotor periaqueductal gray
Su3C	supraoculomotor cap
SubB	subbrachial nucleus
SuG	superficial gray layer of the superior colliculus
ts	tectospinal tract
VLPAG	ventrolateral periaqueductal gray
VLTg	ventrolateral tegmental area
VTA	ventral tegmental area
vtgx	ventral tegmental decussation
VTRZ	visual tegmental relay zone
xscp	decussation of the superior cerebellar peduncle
Zo	zonal layer of the superior colliculus
Medulla	
7N	facial nucleus
10N	dorsal motor nucleus of vagus
12N	hypoglossal nucleus
Amb	ambiguus nucleus
AP	area postrema
CeCv	central cervical nucleus
cu	cuneate fasciculus
Cu	cuneate nucleus
DMSp5	dorsomedial spinal trigeminal nucleus
DPGi	dorsal paragigantocellular nucleus
DPO	dorsal periolivary region
ECu	external cuneate nucleus
EVe	nucleus of origin of efferents of the vestibular nerve
FVe	F cell group of the vestibular complex
Gi	gigantocellular reticular nucleus
GiA	gigantocellular reticular nucleus, alpha part
GiV	gigantocellular reticular nucleus, ventral part
Gr	gracile nucleus
icp	inferior cerebellar peduncle (restiform body)
In	intercalated nucleus of the medulla
InM	intermedius nucleus of the medulla
IOB	inferior olive, subnucleus B of medial nucleus
IOBe	inferior olive, subnucleus B of medial nucleus
IOC	inferior olive, subnucleus C of medial nucleus

IOD	inferior olive, dorsal nucleus
IOK	inferior olive, cap of Kooy of the medial nucleus
IOVL	inferior olive, ventrolateral protrusion
IRt	intermediate reticular nucleus
Li	linear nucleus of the medulla
LPGi	lateral paragigantocellular nucleus
LRt	lateral reticular nucleus
LRtPC	lateral reticular nucleus, parvicellular part
LSO	lateral superior olive
LVe	lateral vestibular nucleus
LVPO	lateroventral periolivary nucleus
MdD	medullary reticular nucleus, dorsal part
MdV	medullary reticular nucleus, ventral part
MVe	medial vestibular nucleus
MVeMC	medial vestibular nucleus, magnocellular part
MVePC	medial vestibular nucleus, parvicellular part
PCRt	parvicellular reticular nucleus
PCRtA	parvicellular reticular nucleus, alpha part
PMn	paramedian reticular nucleus
PPy	parapyramidal nucleus
Pr	prepositus nucleus
Pr5DM	principal sensory trigeminal nucleus, dorsomedial part
Pr5VL	principal sensory trigeminal nucleus, ventrolateral part
PSol	parasolitary nucleus
py	pyramidal tract
pyx	pyramidal decussation
RAmb	retroambiguus nucleus
RMg	raphe magnus nucleus
Ro	nucleus of Roller
ROb	raphe obscurus nucleus
RPa	raphe pallidus nucleus
RVL	rostroventrolateral reticular nucleus
Sol	nucleus of the solitary tract
SolC	nucleus of the solitary tract, commissural part
SolCe	nucleus of the solitary tract, central part
SolDL	solitary nucleus, dorsolateral part
SolDM	nucleus of the solitary tract, dorsomedial part
SolG	nucleus of the solitary tract, gelatinous part
SolI	nucleus of the solitary tract, interstitial part
SolIM	nucleus of the solitary tract, intermediate part
SolM	nucleus of the solitary tract, medial part
SolV	solitary nucleus, ventral part
SolVL	nucleus of the solitary tract, ventrolateral part
sp5	spinal trigeminal tract
Sp5C	spinal trigeminal nucleus, caudal part
Sp5I	spinal trigeminal nucleus, interpolar part
Sp5O	spinal trigeminal nucleus, oral part
Sp5ODM	spinal trigeminal nucleus, oral part, dorsomedial division
Sp5OVL	spinal trigeminal nucleus, oral part, ventrolateral division
SPO	superior paraolivary nucleus
SpVe	spinal vestibular nucleus

SuVe	superior vestibular nucleus
VCA	ventral cochlear nucleus, anterior part
vsc	ventral spinocerebellar tract
X	nucleus X
Cerebellum	
1Cb	1st Cerebellar lobule
2Cb	2nd Cerebellar lobule
3Cb	3rd Cerebellar lobule
4&5Cb	4&5th Cerebellar lobules
6Cb	6th Cerebellar lobule
7Cb	7th Cerebellar lobule
8Cb	8th Cerebellar lobule
9Cb	9th Cerebellar lobule
10Cb	10th Cerebellar lobule
Crus1	crus 1 of the ansiform lobule
Crus2	crus 2 of the ansiform lobule
Fl	flocculus
PFl	paraflocculus
PM	paramedian lobule
Sim	simple lobule
Ventricular zones	
3V	3rd ventricle
OV	olfactory ventricle (olfactory part of lateral ventricle)
OV	olfactory ventricle (olfactory part of lateral ventricle)
SVZ	subventricular zone